INSTITUTO POLITÉCNICO DE BRAGANÇA
Escola Superior de Tecnologia e Gestão

Development of Polymer Networks for The Purification of Stilbenes and Lignans in Pinus Pinea and Pinus Pinaster

Sourour Oesleti

Supervisor: Doctor Rolando Carlos Pereira Simões Dias

Thesis presented to the **Escola Superior de Tecnologia e Gestão – Instituto Politécnico de Bragança,** presented to the institute itself as a requirement for obtaining the **master's degree in chemical engineering**.

October 7, 2025

ACKNOWLEDGMENT

I would like to express my sincere gratitude to my advisor, Professor Dr. Rolando Carlos Pereira Simões Dias from the Polytechnic Institute of Bragança (IPB), for his unwavering support and kind guidance throughout my academic journey. His presence and encouragement were the cornerstone of the completion of this work, and I am deeply thankful for his continuous care and boundless support.

I would also like to thank Professors André Heeres and Erik Keller from Hanze University of Applied Sciences, Netherlands, for their valuable support and contributions.

My gratitude also extends to my colleagues at IPB, particularly PhD students Amir Bzainia and Cláudia Martins, for their valuable collaboration and support throughout the research and laboratory work.

I extend heartfelt thanks and affection to my dear family, who have always been a source of strength and support throughout my academic and professional path.

Finally, I would like to acknowledge the financial support provided by the Foundation for Science and Technology (FCT, Portugal) through national funds FCT/MCTES (PIDDAC) to CIMO (UIDB/00690/2020 and UIDP/00690/2020) and the SusTEC project (LA/P/0007/2020), which made this research possible.

Abstract

This thesis presents a comprehensive study on the use of functionalized polymer networks for the separation and enrichment of lignans from pine extracts, with the goal of valorizing forestry by-products using sustainable techniques. Lignans such as Pinoresinol and its derivatives are bioactive compounds with significant pharmacological interest, found in considerable amounts in the pine trees like Pinus pinaster and Pinus pinea. The crude extract was obtained via ultrasound-assisted extraction using an ethanol/water mixture (80:20 v/v), which ensured a more efficient release of bioactive compounds without compromising their structural integrity. A polymer network based on bis(acrylamido)pyridine was synthesized and used in a sorption/desorption process to selectivity isolate lignans. Elution with a 60:40 ethanol/water mixture allowed a notable enrichment of lignans, with the main compound showing a six-fold enrichment compared to the original crude extract.

The performance of the polymer network was further demonstrated through a two-cycle sorption/desorption process, confirming its reusability and stability, which are essential for real-world applications. The experimental design incorporated several characterization techniques to validate the presence and concentration of lignans in the different fractions. This work not only confirms the viability of using functional polymer networks for the selective enrichment of lignans but also opens the possibility for similar methodologies to be applied to related compounds, such as stilbenes, also present in Pinus by-products. The presented strategy contributes to the development of greener, more efficient purification technologies aligned with the principles of the circular economy.

Resumo

Esta dissertação apresenta um estudo abrangente sobre a utilização de redes poliméricas funcionalizadas para a separação e enriquecimento de lignanos a partir de extratos de pinheiro, com o objetivo de valorizar subprodutos florestais através de técnicas sustentáveis. Lignanos como o pinoresinol e os seus derivados são compostos bioativos de elevado interesse farmacológico, encontrados em quantidades consideráveis em espécies de pinheiro como o Pinus pinaster e o Pinus pinea. O extrato bruto foi obtido por extração assistida por ultrassons, utilizando uma mistura etanol/água (80:20 v/v), que assegurou uma libertação mais eficiente dos compostos bioativos sem comprometer a sua integridade estrutural. Foi sintetizada uma rede polimérica baseada em bis(acrilamido)piridina, utilizada num processo de sorção/dessorção para isolar seletivamente os lignanos. A eluição com uma mistura etanol/água (60:40) permitiu um enriquecimento notável em lignanos, sendo que o composto principal apresentou um enriquecimento seis vezes superior em comparação com o extrato bruto original.

O desempenho da rede polimérica foi ainda demonstrado através de um processo de sorção/dessorção em dois ciclos, confirmando a sua reutilização e estabilidade, aspetos essenciais para aplicações práticas. O desenho experimental incorporou várias técnicas de caracterização para validar a presença e a concentração de lignanos nas diferentes frações. Este trabalho não só confirma a viabilidade da utilização de redes poliméricas funcionais para o enriquecimento seletivo de lignanos, como também abre a possibilidade de aplicar metodologias semelhantes a compostos relacionados, como os estilbenos, também presentes em subprodutos de Pinus. A estratégia apresentada contribui para o desenvolvimento de tecnologias de purificação mais verdes e eficientes, alinhadas com os princípios da economia circular.

Table of Contents

List of figures

List of Tables

Chapter 1 Introduction

The increasing demand for natural bioactive compounds has driven interest in the recovery and valorization of phenolic compounds from underutilized biomass sources, such as forestry residues. Lignans, a class of phenylpropanoid dimers, are among the most biologically active secondary metabolites found in plants. They have attracted significant attention due to their antioxidant, anti-inflammatory, antitumoral, and antiviral properties. These compounds occur naturally in several plant tissues, including seeds, roots, and notably, in the bark of coniferous species like Pinus pinaster and Pinus pinea. The sustainable exploitation of these abundant and renewable resources is essential in the context of green chemistry and the development of bio-based value chains.

Traditional methods of lignan extraction and purification rely heavily on organic solvent extraction followed by multiple chromatographic steps. While effective, these techniques are often laborious, expensive, and generate considerable solvent waste, contradicting the principles of green chemistry. As a result, alternative strategies are being explored to improve the efficiency, selectivity, and environmental performance of the lignan separation process. Among these, polymeric adsorbents have emerged as a promising approach due to their tunable properties, ease of synthesis, and potential for selective recognition of target compounds.

Functional polymer networks, particularly those incorporating recognition motifs such as bis(acrylamido)pyridine), offer enhanced interaction with phenolic compounds through hydrogen bonding and π-π stacking interactions. These properties make them ideal candidates for the selective capture and release of lignans from complex plant extracts. Moreover, their mechanical and chemical stability allows for their reuse in multicycle processes, improving their sustainability and cost-effectiveness.

This work aims to develop Poly(BAAPy), a polymer network synthesized from 2,6-bis(acrylamido)pyridine (BAAPy), as an efficient adsorbent for the purification of lignans, particularly pinoresinol, from Pinus pinea and Pinus pinaster extracts. The polymer was synthesized by free radical polymerization using AIBN as a thermal initiator at 60 °C, with the monomer dissolved in ACN and DMF, yielding about 84% after 24 hours.

To obtain the natural extracts, pine bark was subjected to ultrasound-assisted extraction using an ethanol/water (80:20 v/v) mixture, a solvent system well-suited for polyphenol extraction due to its polarity and compatibility with phenolic compounds. The crude extract, rich in

lignans, was subsequently treated with the BAAPy-based polymer network under controlled sorption/desorption conditions.

Adsorption experiments were performed in packed columns at 20 °C and 1 mL min^{-1} for 24 hours, followed by desorption at 45 °C using various ethanol/water ratios. The 60:40 v/v mixture proved most effective, achieving a sixfold enrichment of pinoresinol, although minor signal losses indicated partial desorption and limited selectivity

Finally, the two-cycle sorption/desorption tests confirmed the robustness and reusability of the polymer network. Overall, these results demonstrate the potential of Poly(BAAPy) as a sustainable adsorbent for lignan purification and provide a foundation for extending this approach to other bioactive polyphenols, such as stilbenes, derived from Pinus subproducts.

This thesis is structured as follows. The first part provides the theoretical background and literature review. The second describes the materials and experimental methods. The third presents the main results and their discussion. The final part concludes the work and outlines future perspectives.

Chapter 2 Theoretical background

Forests have long provided humans with essential materials, from timber to medicinal compounds, yet many of their by-products remain underexploited. Among these, the bark, knots, and needles of coniferous species such as Pinus pinea (stone pine) and Pinus pinaster (maritime pine) are rich in bioactive secondary metabolites. These include phenolic compounds like stilbenes and lignans, which have garnered increasing attention due to their antioxidant, antimicrobial, and potential therapeutic properties. Despite their promising bioactivity, the efficient and selective extraction and purification of these molecules from complex plant matrices pose significant scientific and technical challenges. Conventional extraction techniques often require intensive solvent use and multiple purification steps, which can compromise both sustainability and compound integrity. To overcome these limitations, the development of synthetic sorbent materials, particularly polymer-based networks, has emerged as a promising alternative for the selective recovery of phenolic compounds. Polymers with tailored chemical functionalities have the potential to mimic the specificity of biological recognition systems, offering greater efficiency, reusability, and environmental compatibility. Within this framework, the present thesis explores the design, synthesis, and application of functional polymer networks for the purification of lignans and stilbenes from extracts of Pinus pinea and Pinus pinaster. The approach is grounded in the synthesis of polymer networks via free-radical polymerization, using monomers that can provide both structural stability and interactive functional groups capable of non- covalent binding.

2.1 Pinus pinaster and Pinus pinea

Both Pinus pinaster (maritime pine) and Pinus pinea (stone pine) are members of the Pinaceae family and the genus, which encompasses a wide range of species. Pinus pinaster is particularly noted for its fast growth, typically reaching heights of 20 to 30 meters, with some specimens growing as tall as 40 meters. It is distinguished by a deep trunk, well-developed secondary root system, and thick, reddish-brown bark with deep cracks [1]. During the conversion of Pinus pinaster into pulp, by-products like pine knots are produced. These knots are generally considered undesirable due to their high content of lipophilic compounds [2]. For instance, a French paper mill consumes 1000-2000 tons of pine wood daily, resulting in 10-40 tons of pine knots per day [3]. Although these knots are often used as fuel, they contain high concentrations of polyphenols, including lignans, flavonoids, and stilbenes, making them a valuable potential source of biomass.

The Stone Pine (Pinus pinea), also known as the umbrella pine or pine, typically grows to a height of 20 to 25 meters and is characterized by long, thick, ascending branches that form a dense, spherical crown reaching 40-60 meters in width [4]. The stone pine is renowned for producing edible seeds (pine nuts), which are widely incorporated into traditional Mediterranean cuisine and are highly regarded for their exceptional nutritional and medicinal properties [5].

The most important differences between Pinus pinaster and Pinus pinea are summarized in Table 1.

Table 1: Comparative Characteristics of Pinus pinaster and Pinus pinea

Factor	***Pinus pinea (Stone Pine)***	***Pinus pinaster (Maritime Pine)***
Size and Shape	Medium-sized Dense, rounded crown	Taller Irregular shape
Needles	Shorter, softer	Longer, tougher and rougher
Uses	It is valued for its edible seeds	It is mainly used for soil erosion control.

2.2 Bioactive compounds in Pinus pinaster and Pinus pinea

The Pinus pinaster trees and Pinus pinea contain a variety of bioactive compounds. Phenolic compounds are among the main chemical constituents of these trees and include phenolic acids, flavonoids, stilbenes and lignans. Among these, lignans and stilbenes are present in Pinus species at varying concentrations.

2.2.1 Stilbenes: Structure, Function, Biosynthesis, and Distribution

2.2.1.1 Stilbene Diversity and UV Detection

The UV spectrum of stilbenes is characterized by distinct features that help differentiate them from other phenolic compounds such as lignans. Typically, stilbenes exhibit two well-defined absorption peaks: a major peak (λ_{max}) in the range of 305–325 nm, attributed to the $\pi \rightarrow \pi^*$ transitions within their extended conjugated system, and a secondary peak around 280–290 nm, often associated with phenolic structural components. For example, resveratrol, a representative stilbene, displays a primary absorption maximum near 306–310 nm and a secondary peak close to 284–288 nm. Its spectrum is generally smooth, with clearly separated peaks and a short tail beyond 330 nm. These spectral features result from the conjugated phenyl-ethylene-phenyl (C6–C2–C6) structure and the presence of hydroxyl groups, which enhance absorption in the

UV range. Compared to lignans, which often show more complex and broader spectral patterns with extended tails beyond 240 nm, stilbenes tend to have simpler, dual-peak profiles with sharper definition. Therefore, when analyzing unknown compounds using HPLC-UV or DAD, the presence of these characteristic peaks can be a strong indicator of a stilbene structure.

2.2.1.1.1 Structural diversity of Stilbenes

Stilbenes and stilbenoids are two groups of organic compounds that share a common basic structure but differ in their chemical composition and biological effects. Stilbene is a simple compound made of a 1,2-diphenylethene structure, where two aromatic rings (phenyl groups) are connected by a two-carbon bridge. Stilbene exists in two geometric forms: cis and trans (Figure 1), with the transform being more stable and more common in nature. Stilbenoids, on the other hand, are natural derivatives of stilbene. Plants produce them by adding functional groups such as hydroxyl (OH), methoxy (OCH_3), or even sugar units, which makes stilbenoids more diverse and biologically active [6].

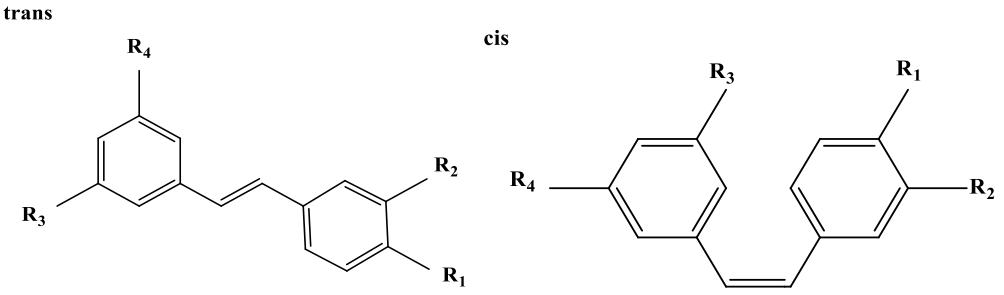

Stilbenes and Stilbenoids	Molecular Formula	R1	R2	R3	R4
Stilbene	$C_{14}H_{12}$	H	H	H	H
trans-Resveratrol	$C_{14}H_{12}O_3$	OH	H	OH	OH
trans-Piceid (Polydatin)	$C_{20}H_{22}O_8$	OH	H	OH	O-glucoside
trans-Piceatannol	$C_{14}H_{12}O_4$	OH	OH	OH	OH
trans-Isorhapontigenin	$C_{15}H_{14}O_4$	OCH_3	OH	OH	OH
trans-Astringin	$C_{20}H_{22}O_9$	OH	OH	OH	O-glucoside
trans-Pinosylvin	$C_{14}H_{12}O_2$	H	H	OH	OH
trans-Pinosylvin-Monomethyl Ether	$C_{15}H_{14}O_2$	H	H	OH	OCH_3
trans-Pinosylvin Dimethyl Ether	$C_{16}H_{16}O_2$	H	H	OCH_3	OCH_3
trans-Dihydropinosylvin Monomethyl Ether	$C_{15}H_{16}O_3$	H	H	OH	OCH_3
trans-Pinosilbene	$C_{15}H_{14}O_3$	H	OH	OH	OH
trans-Pinosilbeneoside	$C_{21}H_{24}O_9$	O-glucoside	OH	OH	OH
trans-Isorhapontigenin	$C_{15}H_{14}O_4$	OH	OCH_3	OH	OH
trans-Isorhapontin	$C_{21}H_{24}O_9$	OH	OCH_3	O-glucoside	OH

Figure 1: Selection of stilbenes and stilbenoids isolated from wood samples [6].

2.2.1.1.2 UV Profiling of Stilbenes Subtypes

Based on the article by Fang et al. (2019), one effective approach for connecting stilbenes through their UV spectra involves examining the shifts in the absorption maxima (λ_max) caused by substituent effects. Stilbenes exhibit characteristic UV absorption patterns that are highly sensitive to the type and position of substituent groups attached to the aromatic rings. For example, electron-donating groups (-OH or -OCH_3…) typically cause a bathochromic shift (red shift) in the range of approximately 10-20 nm, resulting in absorption at longer wavelengths, while electron-withdrawing groups (-NO_2 or -COOH…) induce a hypsochromic shift (blue shift) in the same range, leading to absorption at shorter wavelengths. For instance, a basic stilbene might absorb at around 320-330 nm, while the presence of electron-donating groups could shift the absorption to 340-350 nm [7].

2.2.1.2 Biological Activities of Stilbenes

Stilbenes are a group of phenolic compounds produced by plants as part of their natural defense mechanisms [8]. This is evidenced by the fact that some stlibenes like pinosylvin is not selectively processed in wood, leading to varying concentrations between different parts of the tree. This variation in the distribution of pinosylvin is not random; rather, it serves as clear evidence that its production is linked to defensive needs, as the tree secretes this compound in varying amounts in response to the level of threat or damage in each part. As a consequence, stilbenes exhibit antifungal activity [9], suggesting they can serve as natural pesticides and help reduce the reliance on conventional toxic pesticides. Although stilbenes and stilbenoids are important chemicals in plants and wood, their concentrations are very low. However, this low concentration does not affect their effectiveness, as the concentration of stilbene is linked to a decrease in the half-maximal inhibitory concentration (IC50), which is the concentration that helps reduce biological activity to half of its maximum [10].

Unlike pinosylvin, resveratrol is more uniformly distributed within plants, but it suffers from poor oral bioavailability due to structural changes it undergoes through glycosylation (attachment of sugar units) and oligomerization (formation of larger molecular structures). Additionally, under UV light, its structure can transform into a cyclic compound called 2,4,6-trihydroxyphenanthrene [11].

Besides resveratrol and pinosylvin, there are other active stilbenoid compounds such as astringin (piceatannol, tetrahydroxystilbene), pterostilbene (dimethoxystilbenol), and tetrahydroxystilbene glucoside, which also show promising biological activities. This proves that they possess antioxidant, anti-inflammatory, and antimicrobial properties, making them valuable for various applications [12]. In fact, studies have shown anticancer effects [13] [14], antidiabetic [15], and cardioprotective [16] activities of stilbenes. Thus, stilbenes are used for disease treatments [12] or as ingredients in cosmetic products [17].

2.2.1.3 Biosynthetic pathways of Stilbenes

Stilbene biosynthesis in plants begins with the shikimate pathway, which produces the aromatic amino acids L-phenylalanine and L-tyrosine. These are converted into cinnamic acid and p-coumaric acid, which are then activated by the enzyme 4-coumarate: CoA ligase to form cinnamoyl-CoA and p-coumaroyl-CoA. These CoA-activated compounds then undergo condensation with three molecules of malonyl-CoA, a reaction catalyzed by the enzyme stilbene synthase (STS). This enzyme helps form resveratrol, the central intermediate in stilbene biosynthesis. Resveratrol can be further modified by hydroxylation, methylation, and glucosylation to produce other biologically active stilbenes like astringin and isorhapontin. The process is similar to fatty acid synthesis and occurs mainly in the zone between the phloem and heartwood in trees like Scots pine and Norway spruce. Environmental triggers, such as fungal infections, can increase STS activity and stimulate the accumulation of these defense-related compounds [6].

2.2.1.4 Distribution and Diversity of Stilbenes in the *Pinus* Genus

In the Pinus genus and closely related coniferous species, several types of stilbenes have been reported, reflecting significant chemical diversity depending on the species and the plant part studied. Table 2 presents a comparative overview of stilbene distribution in various Pinus species, as well as in Picea abies (Norway spruce), as documented in the literature.

Table 2: Literature-Based Distribution of Stilbenes in Pinus Species and Picea abies

Ref	Tree Name	Polyphenol Family	Extracted Compounds
[18]	Maritime pine (*Pinus pinaster*)	Stilbenes	Pinosylvin,
			Pinosylvin
			monomethyl ether
[19]	Pinus pinaster (*Maritime pine*)	Stilbenes	Pinosylvin
			Pinosylvin
			monomethyl ether
[20]	Pinus koraiensis (*Korean pine*)	Stilbenes	t-Resveratrol
			t-Piceid
			t-Astringin
			t-Pinostilbenoside,
[21]	Picea abies (*Norway spruce*)	Stilbenes	E-Astringin
			E-Piceid
			E-Isorhapontin
			Z-Astringin
			E-Piceatannol
			Z-Isorhapontin

2.2.2 Lignans: Structure, Function, Biosynthesis, and Distribution

2.2.2.1 Lignan Diversity and UV Detection

2.2.2.1.1 Nomenclature

The term lignan was introduced by Haworth (1936) to describe phenylpropanoid dimers linked through their central carbon (C_8) [22]. Later, Gottlieb (1972) coined neolignane for similar dimers linked differently than $C_8 - C_8'$ (Figure 2).

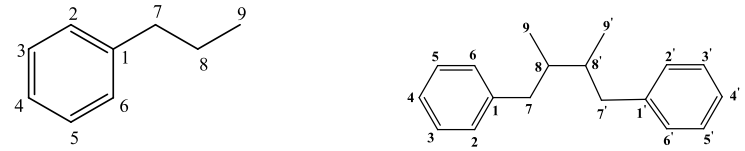

Phenylpropanoid unit Lignan structure

Figure 2: Phenylpropanoid unit and lignan structure*[23]*

2.2.2.1.2 Structural diversity of lignans

To date, a wide range of lignans with various chemical structures and biological activities have been characterized by diverse plants. lignans are classified into eight groups based on their structural patterns, including their carbon skeletons, the way in which oxygen is incorporated into the skeletons, and the cyclization pattern: furofuran, furan, dibenzylbutane, dibenzylbutyrolactol, aryltetralin, arylnaphthalene, dibenzocyclooctadiene, and dibenzylbutyrolactol [24] (Figure 3). In addition, lignans can also occur as mixtures of enantiomers, which are closely associated with their biosynthetic processes and biological activities [25], [26], [27].

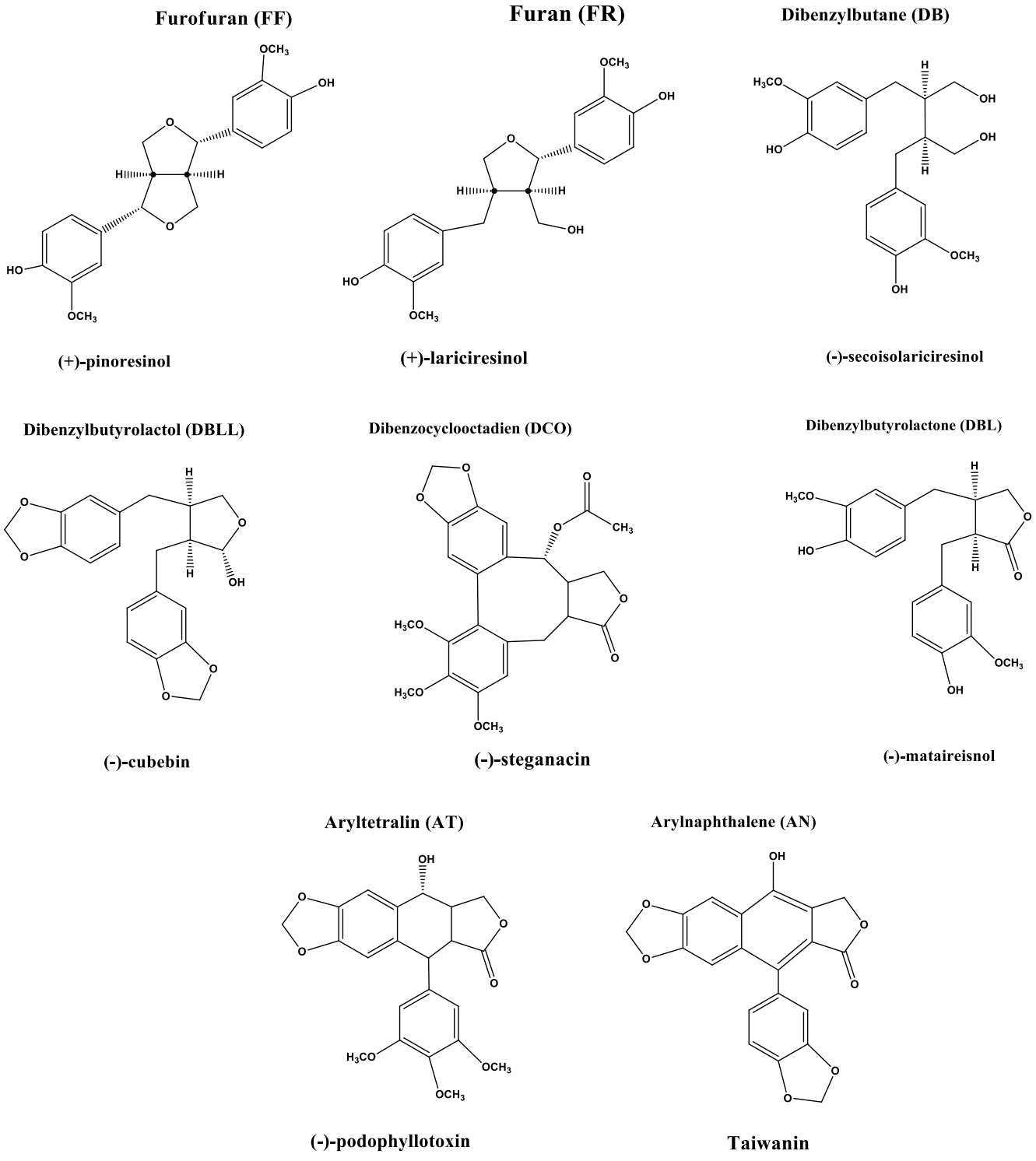

Figure 3: Chemical structures of typical lignans in dietary and medicinal sources [24].

2.2.2.1.3 UV Profiling of Lignans Subtypes

To identify lignans in plant extracts, analyzing their UV spectroscopic patterns is useful. Typically, lignans exhibit three absorption bands at approximately 210, 230, and 280 nm, corresponding to $B^1_{a,b}$, L^1_a, and L^1_b singlet excited states, respectively, as defined by Platt [28]. While the strongest absorption occurs around 210 nm, this peak is rarely recorded. Instead, the bands between 220-240 nm and around 280 nm are more diagnostically valuable and can be tracked throughout the isolation process. Certain lignan subclasses show distinct UV profiles. For instance, arylnaphthalene-type compounds display strong absorption around 260 nm and a broad maximum above 300 nm, making them easy to detect via online UV chromatograms. When chromatograms are recorded simultaneously at 215, 260, and 290 nm, the presence of arylnaphthalenes is indicated by a higher absorbance at 260 nm than at 215 nm. Similarly, dibenzylbutyrolactones show greater absorbance at 290 nm compared to 260 nm, distinguishing them from aryltetralins, which exhibit a decreasing pattern: 215 > 260 > 290 nm. Additionally, butyrolactones can often be differentiated from furofurans/seco-derivatives by their markedly higher absorbance at 290 nm, whereas this difference is less significant in the latter case [29].

2.2.2.2 Biological Activities of Lignans

Several classes of secondary metabolites are synthesized by plants and, among those, lignans are recognized as a class of natural products with a wide spectrum of important biological activities. The major biological actions of lignans are classified into three types: bioactivities on plants, insects, or mammals Table 3 summarizes the main biological properties described in the literature for lignans.

Table 3: Main lignans and their biological activities.

Biological System	***Lignan or Compound***	***Biological Effect***	***Reference***
Insects	(+)-Pinoresinol	Acts as a defensive compound against ants through antifeedant activity in *Pieris rapae* caterpillars	[30]
	Pinoresinol, Hinokinin, Podophyllotoxin	Exhibit pyrethrum-synergistic and antifeedant effects on insects	[31]
	(−)-Lariciresinol	Strongly inhibits lettuce germination	[32],[33]

Plants	(−)-Lariciresinol	Inhibits root growth of Italian ryegrass by 51–55%	[32]
Mammals	Lignans (general)	Metabolized into enterodiol and enterolactone by gut microflora (known as "enterolignans" or "mammalian lignans")	[34], [35]
	Enterolignans	Considered "phytoestrogens" due to weak estrogen-like activity	[36],[37]
	Enterolignans	Bind to estrogen receptors ERα and ERβ	[38],[39]
	Lignans	Show anticancer effects: tumor suppression, angiogenesis inhibition, apoptosis induction, SHBG production	[40], [41], [42], [43]
	Enterolignans	Reduce breast cancer risk and improve prognosis in postmenopausal women	[41],[44],[45] , [46], [47], [48], [49]
	Enterolactone	Serum levels correlate with improved breast cancer prognosis in postmenopausal women	[50]
	(+)-Lariciresinol	Suppresses tumor growth and angiogenesis in MCF-7 xenografts and carcinogen-induced tumors in rats	[42]
	(−)-Secoisolariciresinol diglucosides	Inhibit breast cancer cell proliferation and induce apoptosis	[51]
	Sesamin	Reduces MAPK pathway signaling; more effective in suppressing tumor growth than SDG	[52]
Lifestyle Diseases	Flaxseed lignans	Lower plasma glucose and type 2 diabetes markers after 3 months of supplementation	[53]
	(+)-Sesamin & its digests	Exhibit antihypertensive and antioxidant effects	[54], [55], [56]
	(+)-Sesamin	Protects the liver from oxidation by alcohol, lipids, and free radicals	[54],[57]

	(+)-Pinoresinol	Reduces IL-6 and PGE2 levels and inhibits Cox-2, demonstrating strong anti-inflammatory effects	[35]
	(−)-Matairesinol	Increases Cox-2-derived PGE2 production	[35]

2.2.2.3 Biosynthetic pathways of lignans

Lignan biosynthesis in plants starts from the shikimic acid pathway, which produces the aromatic amino acids L-phenylalanine and L-tyrosine. These are converted into cinnamic acid derivatives, then reduced to three main alcohols: p-coumaryl alcohol, coniferyl alcohol, and sinapyl alcohol. These alcohols are oxidized by the enzyme peroxidase, forming stable free radicals that can couple together to produce primary lignan compounds. Through selective coupling, assisted by a dirigent protein, pinoresinol is formed from two coniferyl alcohol units. This compound is then enzymatically converted to lariciresinol, and then to secoisolariciresinol, which serves as a precursor to more complex lignans like matairesinol and yatein. These in turn lead to the formation of biologically active compounds such as cubebin and podophyllotoxin [23].

2.2.2.4 Lignans Distribution and Diversity in Softwood Species

Softwood, such as Pinus pinaster, which is widely found in Atlantic and Mediterranean regions of Europe, especially in northwest Spain, are among the most important lignocellulosic materials in the Northern Hemisphere [58] [59]. They are composed of structural components (cellulose, hemicellulose, and lignin) and non-structural ones like extractives, which include lignans, phenolic compounds produced by the plant's secondary metabolism. Lignans are key extractives in Pinus pinaster, requiring a better understanding of their spectroscopic properties, especially because softwood species produce a wide variety of them (Table 4). Compounds such as isolariciresinol, pinoresinol, matairesinol, nortrachelogenin, and secoisolariciresinol show maximum absorption between 281 and 290 nm in UV-vis spectroscopy, indicating the absence of conjugated double bonds like C=C or C=O. Lignan composition varies between species. For example, nortrachelogenin is the main compound in Pinus pinaster (11.3%, w/w) [60], while spruce Knots mainly contain HMR, making up 65-85% of their lignan content. The yield and composition of extractives depend on factors like the raw material type, sampling method, and processing conditions. Studies have analyzed wood samples from sapwood, heartwood, and knots, revealing that knots in some softwoods contain high concentrations of lignans [61] [62].

Reference	Tree Name	Compound	Purified Compounds
[60]	Maritime pine (Pinus pinaster)	Fundamental lignans	Pinoresinol
			Matairesinol
			Isolariciresinol
			Secoisolariciresinol
			Nortrachelogenin
[63]	Pinus pinaster (Maritime pine)	Fundamental lignans	Lariciresinol
		Lignan derivatives	Nortrachelogenin guiaicylglyceryl ether
			Hydroxymatairesinol
			Allohydroxymatairesinol

Table 4: Literature-Based Distribution of lignans in Pine Knot Extract (Pinus pinaster)

2.3 Free radical polymerization

The traditional mechanism of free radical polymerization consists of three key stages: initiation, propagation, and termination via a bimolecular process. Free radicals are highly reactive chemical entities containing an unpaired electron. They can be generated through physical methods such as thermal excitation and irradiation or via chemical processes like oxidation-reduction and addition, which involve the homolytic cleavage of covalent bonds [64]. This technique is mainly used for polymerizing monomers with the general structure CH2=CR1R2, as it does not require highly pure reagents or strict control over the exclusion of moisture, oxygen, or other impurities. Moreover, these reactions can be conducted under mild conditions, such as ambient temperature and atmospheric pressure, either in the bulk phase or in solution. However, the molecular weight distribution resulting from free radical polymerization may not be optimal for certain polymer applications.

In the 1990s, the concept of reversible-deactivation radical polymerization (RDRP), also known as controlled or living free radical polymerization, was introduced. This technique allows minimizing unwanted termination reactions and achieving better control over molecular weight distribution, resulting in enhanced polymer properties such as solubility, viscosity, and thermal stability. Moreover, it expands the potential for vinyl polymers and improves control over their structure and final characteristics [64] [65].

2.3.1 Initiation

The first stage of free radical polymerization is known as the initiation phase. During this stage, free radicals, which are highly reactive molecules with an unpaired electron, are generated. The process typically begins with an initiator, such as peroxides or azo compounds, which decompose under heat or radiation to produce free radicals. These radicals then react with monomer molecules, forming an active radical that stimulates the growth of the polymer chain. This stage marks the beginning of the reaction, allowing the chain to continue growing and developing until it eventually reaches the termination phase [66].

2.3.2 Propagation

Propagation in free radical polymerization (FRP) is the phase where the polymer chain expands following the initiation step. During this stage, the free radical generated in the initiation process reacts with additional monomer molecules, resulting in the incorporation of a new monomer unit into the growing polymer chain. This process occurs quickly and in a step-by-step manner, extending the polymer chain until the monomers are depleted or termination mechanisms are triggered [65], [66].

2.3.3 Termination

Termination in free radical polymerization is the final stage, during which the growth of polymer chains stops, bringing the reaction to an end. This process usually occurs through two primary mechanisms: combination (coupling) and disproportionation. In the combination mechanism, two polymer chains, each containing a free radical, react to form a single, longer, inactive chain, resulting in a polymer with a higher molecular weight. In the disproportionation mechanism, a hydrogen atom is transferred from one chain to another, producing two distinct polymers, one with a saturated end and the other with an unsaturated end.

2.3.4 Controlled Radical Polymerization (CRP)

(CRP) is an advanced technique designed to enhance control over polymer chain growth during radical polymerization by minimizing unwanted termination reactions and reducing chain transfer. Unlike conventional radical polymerization, which often results in a broad molecular weight distribution, CRP enables the synthesis of polymers with more uniform molecular weights and improved properties. The three primary methods of CRP include reversible addition-fragmentation chain transfer (RAFT) polymerization, atom transfer radical polymerization (ATRP), and nitroxide-mediated polymerization (NMP). Each approach utilizes a distinct mechanism to regulate polymer chain growth, whether by transferring activity between chains, as seen in RAFT, or through reversible activation and deactivation processes, as employed in ATRP. These advancements have made it possible to design polymers with precise and customizable functions, paving the way for innovative applications in pharmaceuticals, nanomaterials, and biosensors [67].

2.4 Structural and Functional Role of 2,6-Bis(acrylamido)pyridine in Free Radical Polymerization Networks

The inclusion of the chemical structure of the functional monomer 2,6-bis(acrylamido)pyridine (or 2,6-BAP) is essential due to its pivotal role in the formation of polymeric networks. This monomer is characterized by its unique structure, which consists of a pyridine ring substituted at positions 2 and 6 with two acrylamide groups (Figure 4). These groups are highly reactive toward free radical polymerization, owing to the presence of carbon-carbon double bonds (C=C) that enable rapid and efficient polymerization. This chemical reactivity is further enhanced by the nitrogen atom in the pyridine ring, which possesses a lone pair of electrons capable of engaging in hydrogen bonding or coordination interactions with template molecules or metal ions [68]. Such interactions contribute significantly to the structural stability and selectivity of the resulting polymer matrix. In some cases, these non-covalent interactions may reduce or even eliminate the need for extensive use of cross-linking agents, as they can effectively stabilize the three-dimensional polymeric network. Moreover, the pyridine ring, in conjunction with the acrylamide groups, offers multiple active sites for effective interactions with target molecules such as lignans and stilbenes, especially those bearing polar groups like hydroxyl or methoxy functionalities. These interactions, mainly hydrogen bonding and electrostatic interactions, play a crucial role in forming cavities with specific shapes and chemical environments within the polymer matrix, thereby enabling highly selective molecular

recognition. Thus, understanding the chemical structure of this monomer is not only important for elucidating the polymerization mechanism but also for evaluating its reactivity and ability to bind target molecules. Additionally, the conjugated electronic system of the pyridine ring, combined with the phenyl functional groups, enhances the formation of a three-dimensional polymeric network with high chemical and mechanical stability, making it well-suited for applications such as purification and selective adsorption. In summary, 2,6-BAAP is a promising monomer for the [69]design of advanced functional polymers with high specificity and selective recognition capabilities, supporting its use in various environmental, pharmaceutical, and analytical applications.

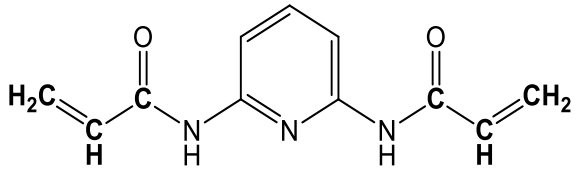

Figure 4: Chemical Structure of 2,6-Bis(acrylamido)pyridine [69].

Chapter 3 Materials And Experimental Methodology

3.1 Materials

Dimethylformamide (DMF, ≥ 99%) was sourced from Acros Organics (Belgium). Dichloromethane (DCM, 99.8%) and ethyl acetate (≥ 99%, used in the BAAPy synthesis) were obtained from Thermo-Scientific (Netherlands), while heptane (technical grade) was acquired from BOOM (Netherlands).

Regarding the main reagents, acryloyl chloride (97%) and 2,6-diaminopyridine (98%) were purchased from Sigma-Aldrich (Netherlands). Triethylamine (TEA, 99%) was supplied by Acros Organics (Netherlands), and 2,2'-azobis(2-methylpropionitrile) (AIBN, ≥ 98%) was purchased from Sigma-Aldrich (Germany).

Finally, ultrapure water used throughout the experiments was obtained from the local laboratory's water purification system.

3.2 Synthesis of 2,6-bis(acrylamido)pyridine

At the start of the experiment, all glassware was dried using air to remove any moisture and avoid any side reactions with the acryloyl chloride (AC). Then, a solution of 2,6-diaminopyridine at a concentration of 0.120 mol/L was prepared in dichloromethane (DCM) inside a round-bottom flask with three openings.

Triethylamine (TEA) was then added at a concentration of 0.264 mol/L (equal to 2.2 equivalents) with strong stirring to ensure good mixing. After that, acryloyl chloride was added slowly using a pressure-equalizing funnel, at a controlled flow rate of 0.147 equivalent per minute, until a total of 2.2 equivalents was added.

The reaction mixture was stirred for 24 hours, while the flask was covered with aluminum foil to protect it from light. A thermometer was placed inside the flask to monitor temperature changes during the reaction. After 24 hours, a clear and homogeneous solution was obtained. Thin layer chromatography (TLC), using a mixture of heptane and ethyl acetate (1:1), confirmed that the reaction was complete and the desired monomer BAAPy was formed.

Next, the reaction mixture was washed with water while stirring in the same flask, causing the BAAPy to precipitate as a solid. The solid was collected using a Büchner funnel and recrystallized using a mixture of ethyl acetate and heptane (2:1), resulting in large crystals. The flask was then cooled at 9°C to help slow crystallization and improve purity. Finally, the

solvent mixture was removed under vacuum, and the crystals were dried. The reaction yield was 80% (equal to 112 mmol or 24.30 grams) [70] .

3.3 Polymerization of BAAPy

The synthesized BAAPy monomer was subjected to free-radical polymerization. A solution of BAAPy was prepared in a solvent mixture of ACN and DMF at a 7:3 volume ratio, with a final concentration of 0.4 mol L^{-1}. to this solution, AIBN was added at 5% molar ratio relative to BAAPy. The reaction mixture was then purged with argon gas for five minutes to remove dissolved oxygen, after which it was transferred to a paraffin oil bath preheated to 60°C. polymerization was carried out for 24 hours, during which the formation of the polymer became visibly apparent. Upon completion, the product was washed thoroughly with methanol and dried, resulting in a fine powder composed of discrete microparticles without signs of bulk aggregation. The final yield of polymerization was approximately 84%. The resulting poly(BAAPy) polymer was subsequently characterized using FTIR spectroscopy as previously described [70].

3.4 Processing of Bioactive Compounds from Pine Extracts

3.4.1 Extract Preparation

Phenolic compounds were extracted from various parts of Pinus pinea and Pinus pinaster trees using either acetonitrile (ACN) or ethanol/water (80:20) mixtures as solvents. In each case, a defined amount of finely ground plant material was subjected to ultrasound-assisted extraction using a SONO SWISS (SW1) device. This was followed by magnetic stirring at room temperature under light-protected conditions. The resulting extracts were then filtered under vacuum to remove any solid residues and ensure clarity for subsequent analytical procedures (Figure 5). The specific extraction conditions, including plant source, sample mass, solvent volume and type, and stirring time, are summarized in Table 5.

Figure 5: extract preparatio

Table 5: Comprehensive details related to the samples

sample	Vegetable source	Mass (g)	Volume of Solvent (mL)	Time of stirring (h)	solvents	HPLC Method	Time of extraction
E1	needles of Pinus pinea tree	5	50	2	ethanol/water 80:20	NATAC	5 minutes
E2	branches of Pinus pinea tree	5	50	1	ethanol/water 80:20	Linear method	5 minutes
E3	bark of Pinus pinaster tree	5	50	1	ethanol/water 80:20	Linear method	5 minutes
E4	bark of Pinus pinaster tree	5	50	1	ACN	Linear method	5 minutes
E5	senescent needles of Pinus pinea tree	3	60	1	ACN	Linear method	5 minutes
E6	Emergent needles of Pinus pinea tree	3	60	1	ACN	Linear method	5 minutes
E7	bark of Pinus pinaster tree	25	125	1	ethanol/water 80:20	Linear method	0.5 h
E8	bark of Pinus pinaster tree	25	125	1	ACN	Linear method	0.5 h

3.4.2 Characterization of phenolic compounds by HPLC-DAD

The Sample were analyzed using a High-Performance Liquid Chromatography (HPLC) system. The HPLC system (KNAUER) consisted of a gradient pump (P6.1) equipped with a degasser, an autosampler (6.1 L), a column thermostat (CT2.1) and a diode array detector (6.1 L). ClarityChrom was the software allowing the control of the HPLC system. The chromatographic analysis was performed using an ascentis C18 (SUPELCO) column with a particle size of 5 µm and dimension 25 cm × 4.6 mm. A solvent gradient was used as the mobile phase, with two distinct elution strategies applied using the HPLC system for the analysis of the extracts. The first method, known as the Fast Gradient (NATAC), involves a rapid transition from a high concentration of acetonitrile (ACN) to a high concentration of water over a short period of approximately 30 minutes. This method is characterized by its quick separation capabilities, making it suitable for preliminary screening or for separating low-polarity compounds. The second method, referred to as the Slow Precise Gradient (linear method), involves a longer gradient lasting about 45 minutes, starting from 90% ACN and gradually decreasing to 10%. This approach offers higher resolution and is especially useful for analyzing polar compounds or complex mixtures. Figure 6 illustrates the fast gradient profile of the first method and the extended gradient program of the second method. The flow rate of the chromatographic analysis was 1 mL/min, and the temperature of the column was set at 45°C.

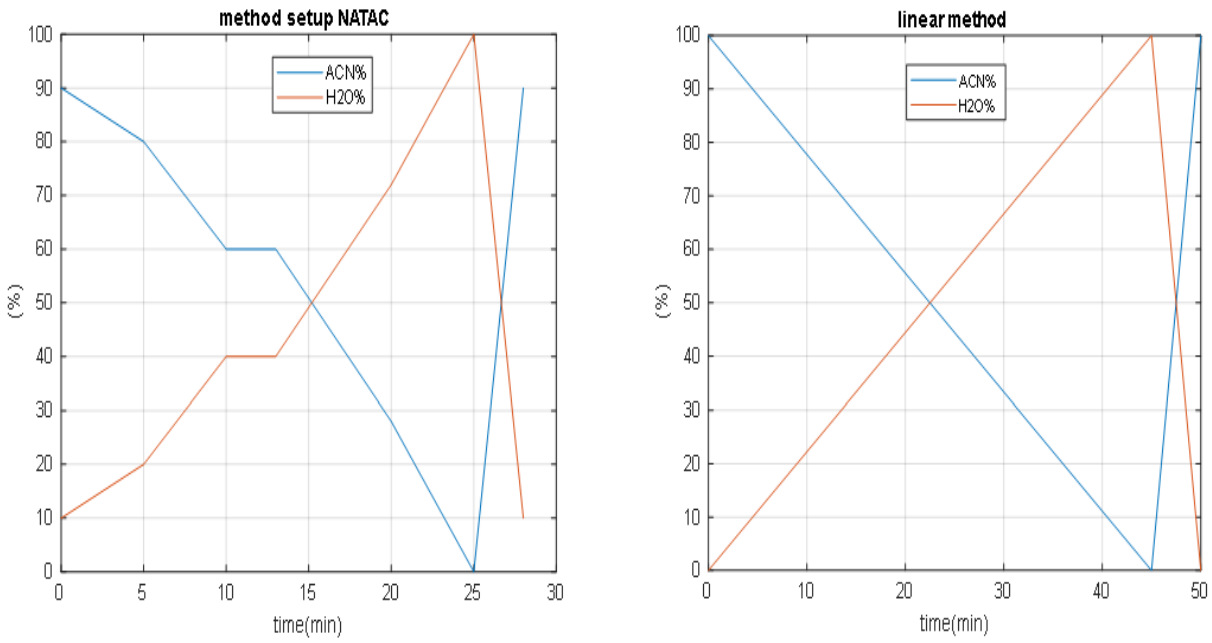

Figure 6: Gradient Elution Profiles Used for HPLC Analysis of Extracts

3.4.3 Designing and running of a pilot size sorption/desorption prototype

Sorption/desorption experiments were conducted using a continuous process prototype to study the ability of the Polymer Network to capture lignans and stilbenes from the extract of Pinus pinaster bark E4. Initially, the experiment was carried out using an empty column with a length of 50 mm and a diameter of 4.6 mm, which was initially packed with 375 mg of the synthesized adsorbent. Subsequently, the packed stainless-steel chromatography column was placed in the continuous process prototype. The column was first cleaned and conditioned using the same solvent employed during the loading process (ACN). Subsequently, E4 was percolated through the column, followed by the necessary steps for recovery and cleaning. Four-way valves were employed to pipe the extract and the desorption solvents to the columns during the sorption/desorption cycles. The temperature of the sorption/desorption columns was controlled within a typical operating range of 15-25 °C for sorption and 45-60 °C for desorption the processes. The prototype also includes a binary pump to produce the change of the solvent composition along with the desorption process. Two reservoirs, each containing solvents with predefined reference compositions, were used to provide the necessary supply for this gradient pump. All parameters, including flow rate, temperature, valves positions, experiments execution and UV data acquisition were controlled using LabVIEW software. The prototype is

also equipped with a fraction collector (LAMBDA OMNICOLL) facilitating the recuperation of the desorbed fractions.

A schematic diagram of the continuous sorption/desorption prototype developed and used for these experiments is presented in figure 7.

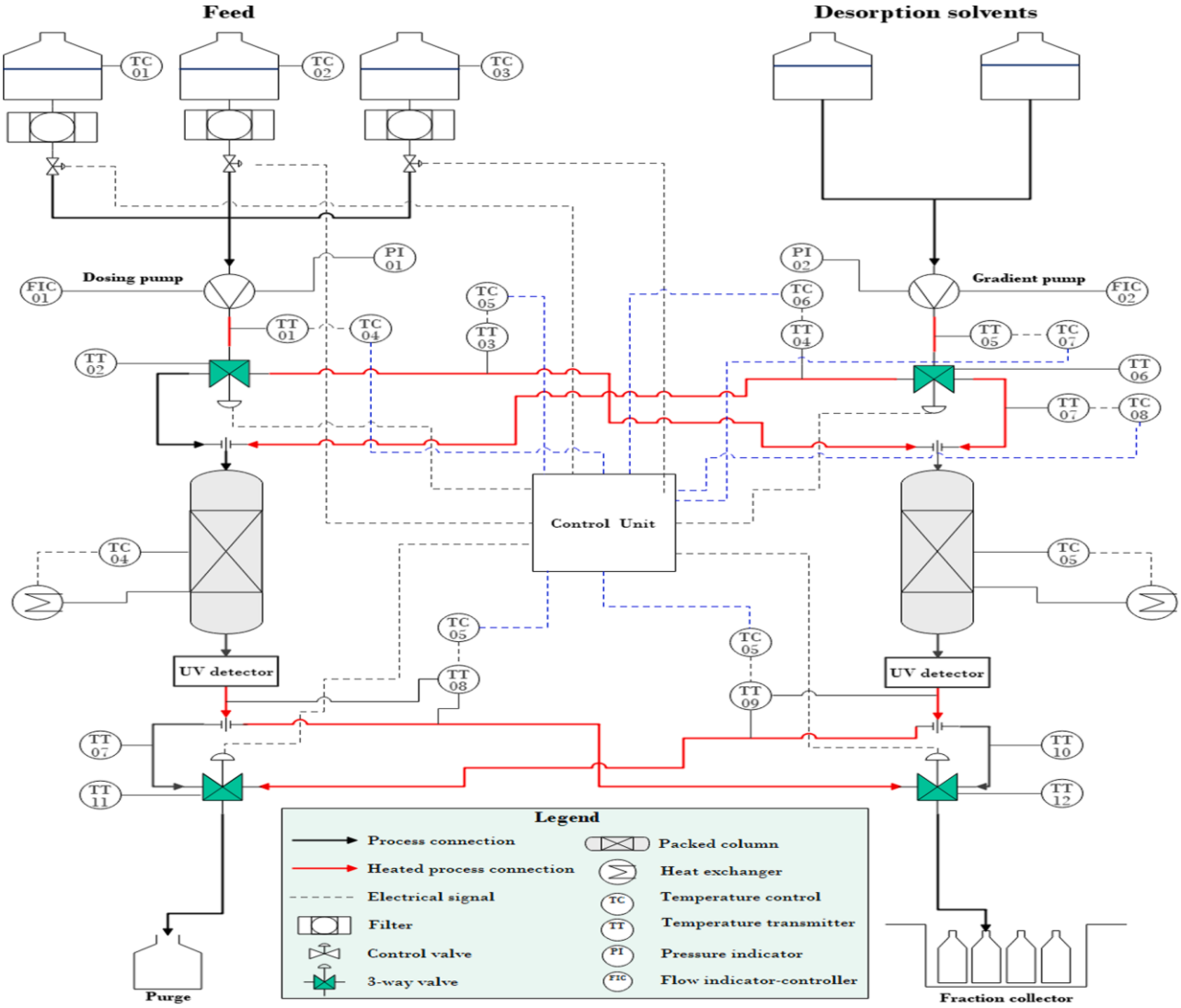

Figure 7: Schematic diagram of the pilot size sorption/desorption prototype used in this work [71].

Chapter 4 Results And Discussion

4.1 Sorbent Characterization (FTIR)

4.1.1 BAAPy monomer synthesis

In this spectrum (Figure 8), the first objective is to confirm the presence of the pyridine ring in the monomer structure. This is evident from the peak at approximately 1600 cm^{-1}, which corresponds to the stretching vibration of the aromatic C=C bond within the ring, accompanied by a peak at around 806 cm^{-1} that reflects the out-of-plane bending vibrations of the aromatic C–H bond, clearly indicating the presence of the ring in the structure. The second objective is to confirm the presence of the amide group in the monomer. This is shown by the strong peak at approximately 1679 cm^{-1}, resulting from the stretching vibration of the C=O bond characteristic of the amide group, along with accompanying peaks such as N–H stretching between 3200–3400 cm^{-1} and N–H bending at around 1550 cm^{-1}. The third objective is to identify the presence of the vinyl group in the monomer structure. This is represented by the peak at approximately 1635 cm^{-1}, which corresponds to the stretching vibration of the aliphatic C=C bond characteristic of vinyl groups.

The new monomer BAAPy is bifunctional, acting as both a functional monomer and a crosslinker, because it contains two acrylamide groups, each with a polymerizable C=C double bond. This bifunctional structure allows each molecule to connect to two different polymer chains during the reaction, leading to the direct formation of a self-crosslinked polymer network during polymerization without the need for external crosslinking agents, as is the case with monofunctional monomers. The new monomer provides also the polymer network with a high density of active sites (Figure 9) capable of forming strong and stable hydrogen bonds with phenolic compounds. With five hydrogen bonding sites derived from its amide groups and pyridine ring, the resulting polymer achieves high adsorption efficiency and selectivity, making it suitable for advanced adsorption-desorption application.

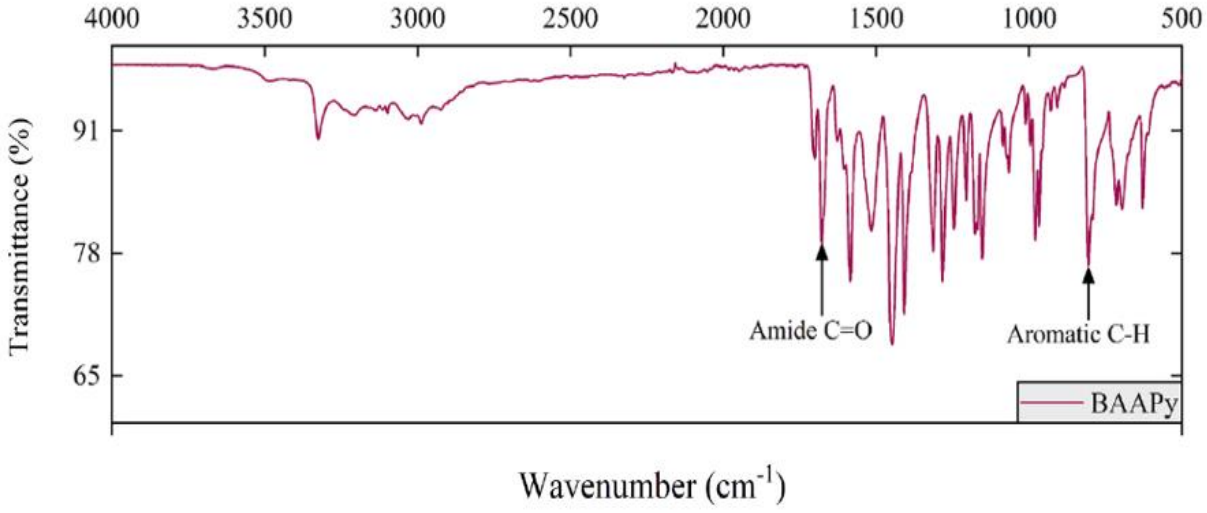

Figure 8: FTIR of the monomer 2,6-bis(acrylamido) pyridine

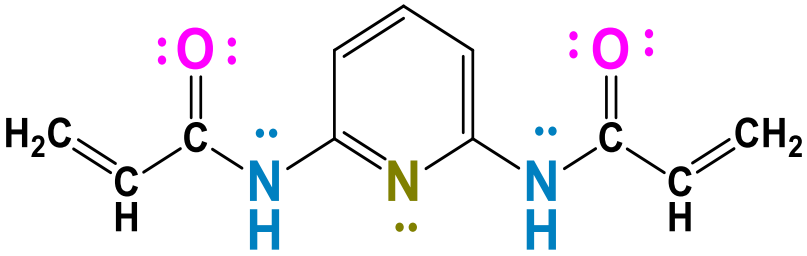

Figure 9: Molecular structures of 2,6-bis(acrlyamido)pyridine (BAAPy), with hydrogen bonding sites highlighted in different colours.

4.1.2 Poly(BAAPy) synthesis

To confirm the polymerization of the monomers, Fourier-transform infrared spectroscopy (FTIR) was carried out in attenuated total reflectance (ATR) mode between 4000 cm^{-1} and 450 cm^{-1} to the dried Polymer Networks synthesized with the functional monomer 2,6-bis(acrylamido)pyridine and the obtained spectra are shown in figure 10.

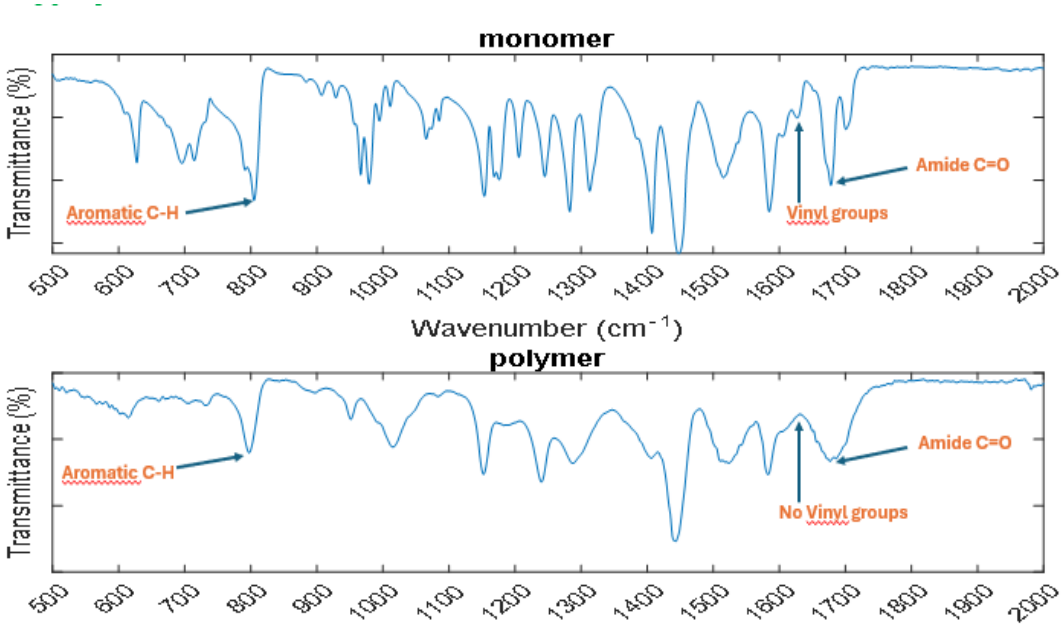

Figure 10: FTIR analysis of Polymer Networks synthesized with the functional monomer 2,6-bis(acrylamido) pyridine and FTIR of the monomer 2,6-bis(acrylamido) pyridine

The FTIR analysis of both the BAAPy monomer and its polymer, poly(BAAPy), shows that the amide group remains intact after polymerization, as the absorption band corresponding to the carbonyl group (C=O) appears in both spectra at around 1679 cm^{-1}. However, a clear broadening of this band is observed in the polymer spectrum, indicating a significant change in the chemical environment surrounding this group, resulting from its involvement in hydrogen bonding interaction with other polymer chains. Such interactions lead to environmental and electronic variability around the C=O groups, causing them to vibrate at slightly different frequencies and producing a broader spectral band. In addition, a decrease in the in the intensity of the out-of-plane bending band of aromatic C-H bonds at around 806 cm^{-1} is observed after polymerization, indicating that the pyridine ring remains present but is affected by structural changes due to restricted vibrational mobility and changes in the electronic distribution within the molecule. Conversely, the signal at approximately 1600 cm^{-1}, corresponding to the stretching vibrations of aromatic C=C bonds in the pyridine ring, remains unchanged before and after polymerization, confirming the preservation of monomer's aromatic structure and its incorporation into the polymer network without significant modifications. Moreover, the vinyl group peak (~1635 cm^{-1}) present in the monomer spectrum disappears in the polymer spectrum, indicating complete conversion of the vinyl groups during thermal polymerization. This behavior can be explained by the free radical polymerization mechanism, in which heating the

initiator AIBN causes the cleavage of the N=N bond, generating highly reactive free radicals that attack the C=C double bonds of the monomers. The weaker π bond is broken, a new C–C bond is formed between the radical and one carbon atom, while the other carbon becomes a new radical. This process repeats sequentially, converting all double bonds into single C-C bonds and enabling the growth of long polymer chains and the formation of an interlinked polymeric network with a more complex structure than the original monomer.

4.2 Comparison Between the Different Extracts

To analyze the phenolic fingerprints of the different extracts, each sample was subjected to high-performance liquid chromatography coupled with a diode array detector (HPLC-DAD). A three-dimensional chromatogram was generated (Figures 11, 12, 13, 14, 15, 16, 17, 18) to visualize the composition and intensity of the phenolic compounds. Additionally, comparative two-dimensional chromatograms (Figures 19 and 20) were constructed to provide a direct visual comparison between the different extracts, enabling a clearer assessment of the similarities and differences in their phenolic content.

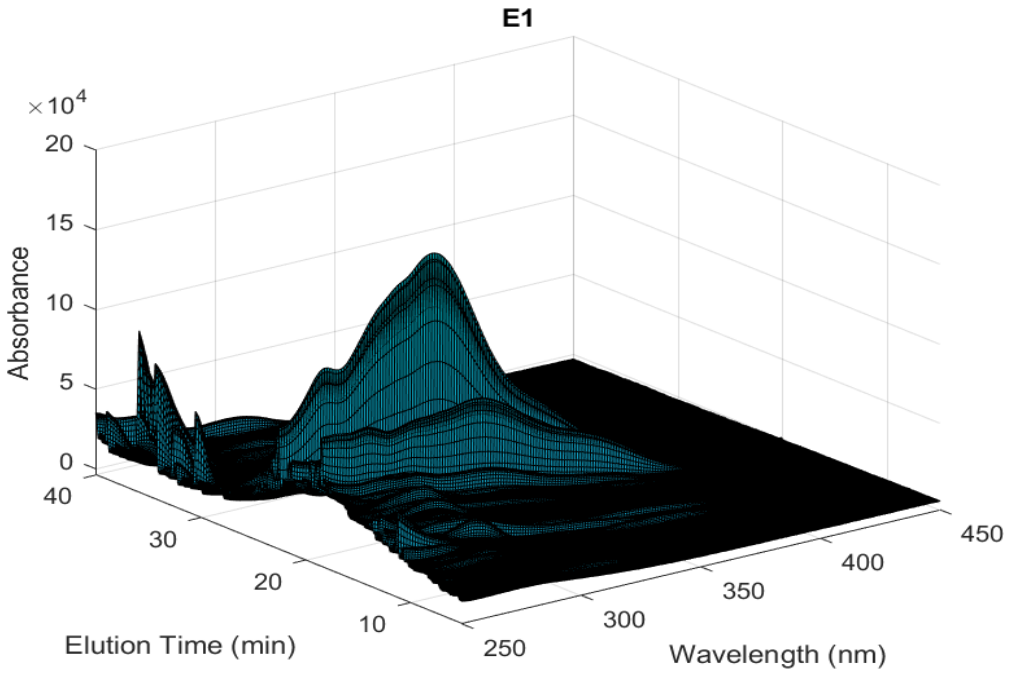

Figure 11: 3D HPLC-DAD chromatogram for the needles of Pinus pinea tree extract obtained according to the conditions in table 5.

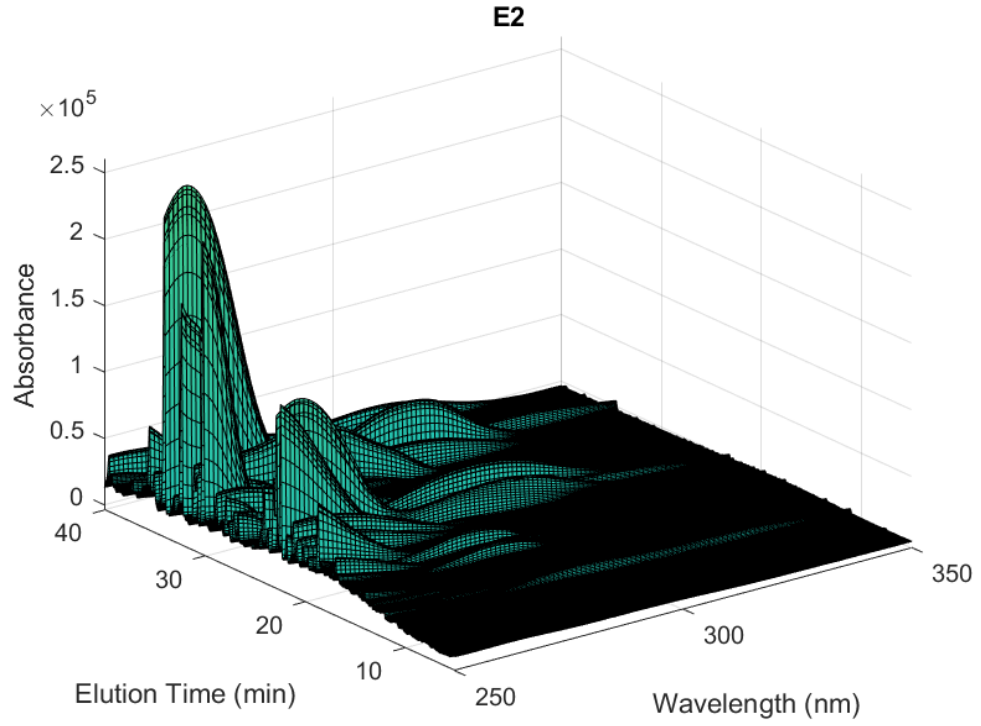

Figure 12: 3D HPLC-DAD chromatogram for the branches of Pinus pinea tree extract obtained according to the conditions in table 5.

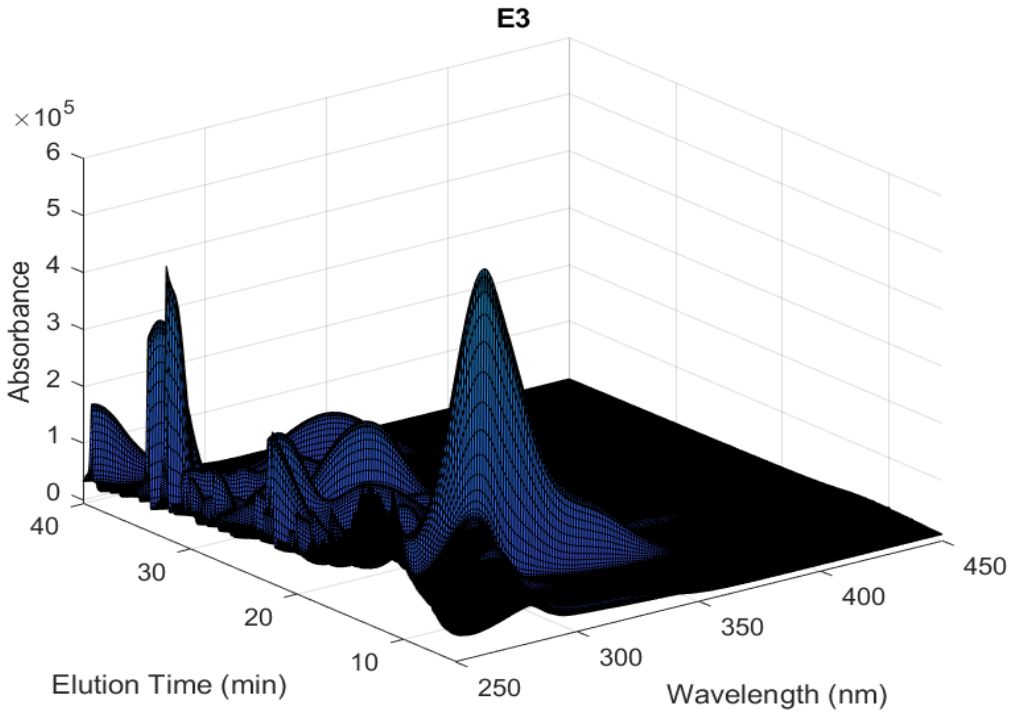

Figure 13: 3D HPLC-DAD chromatogram for the bark of Pinus pinaster tree extract obtained according to the conditions in table 5.

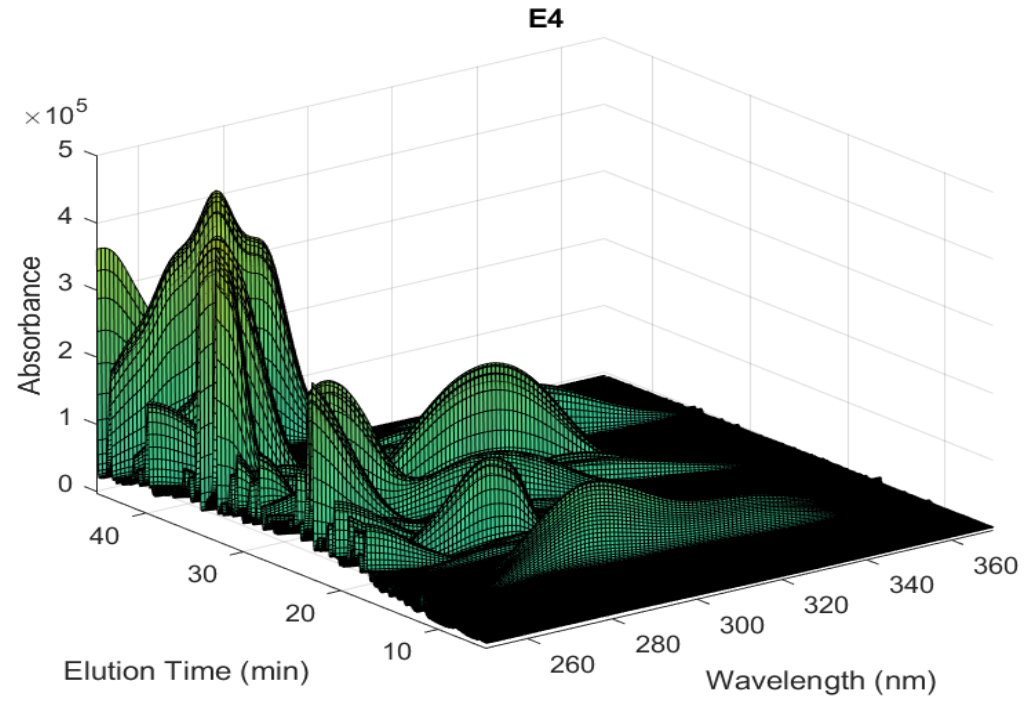

Figure 14: 3D HPLC-DAD chromatogram for the sheets of Pinus pinaster tree extracted according to the conditions in table 5.

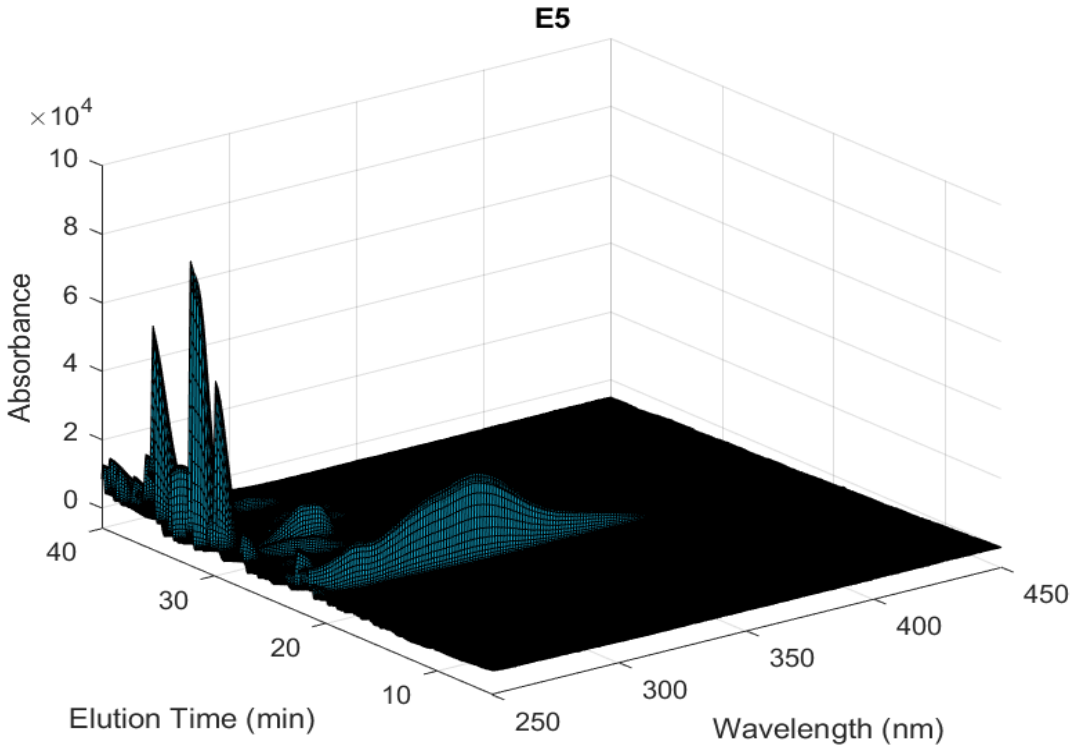

Figure 15: 3D HPLC-DAD chromatogram for the needles of Pinus pinea tree extract obtained according to the conditions in table 5.

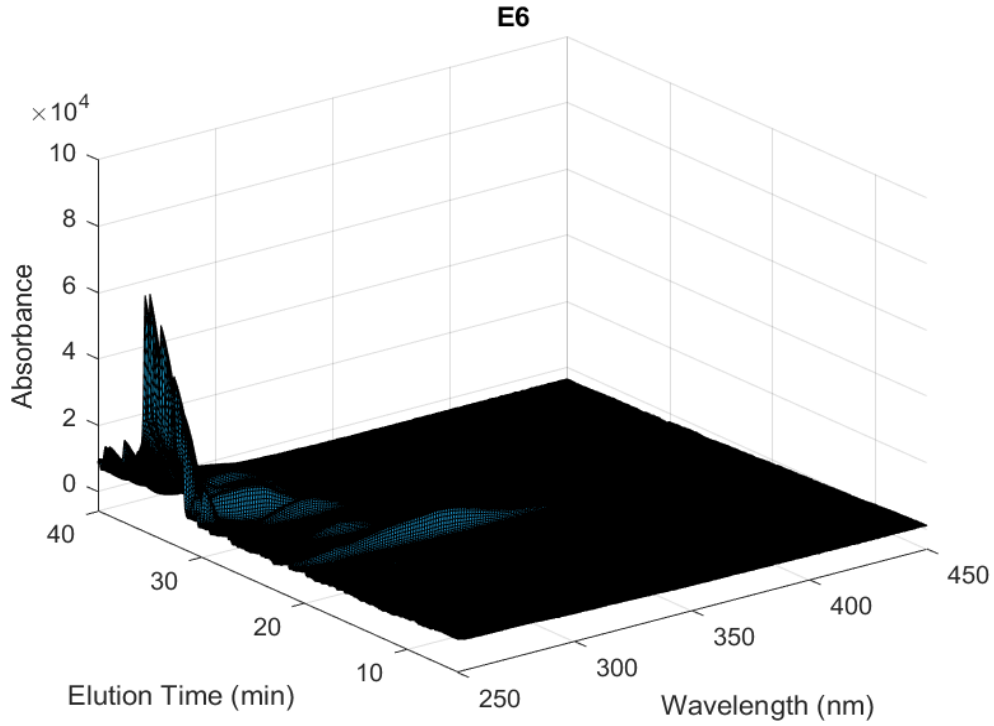

Figure 16: 3D HPLC-DAD chromatogram for the needles of Pinus pinea tree extract obtained according to the conditions in table 5.

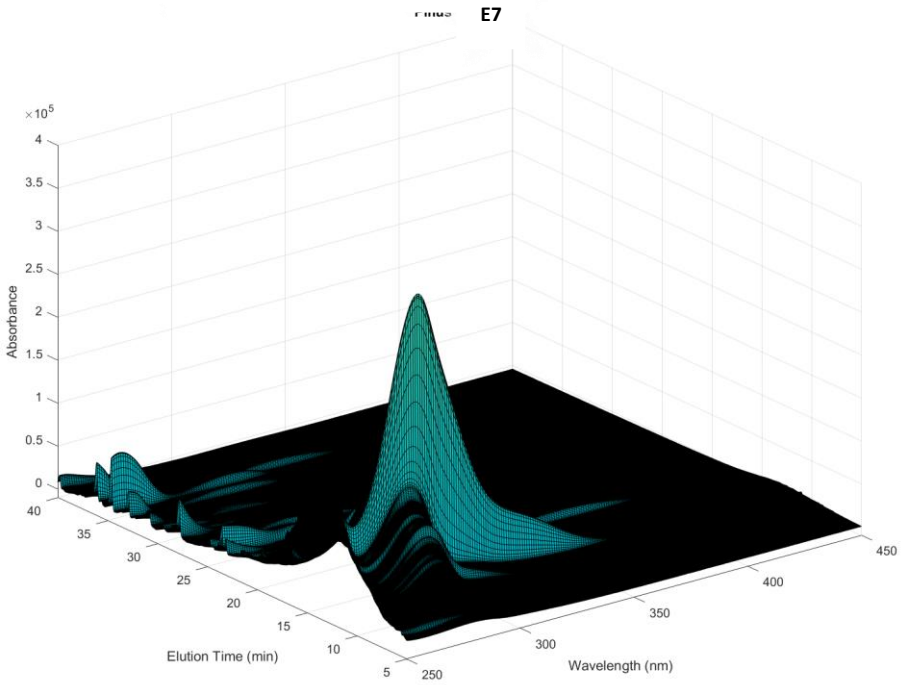

Figure 17: 3D HPLC-DAD chromatogram for the bark of Pinus pinaster tree extract obtained according to the conditions in table 5.

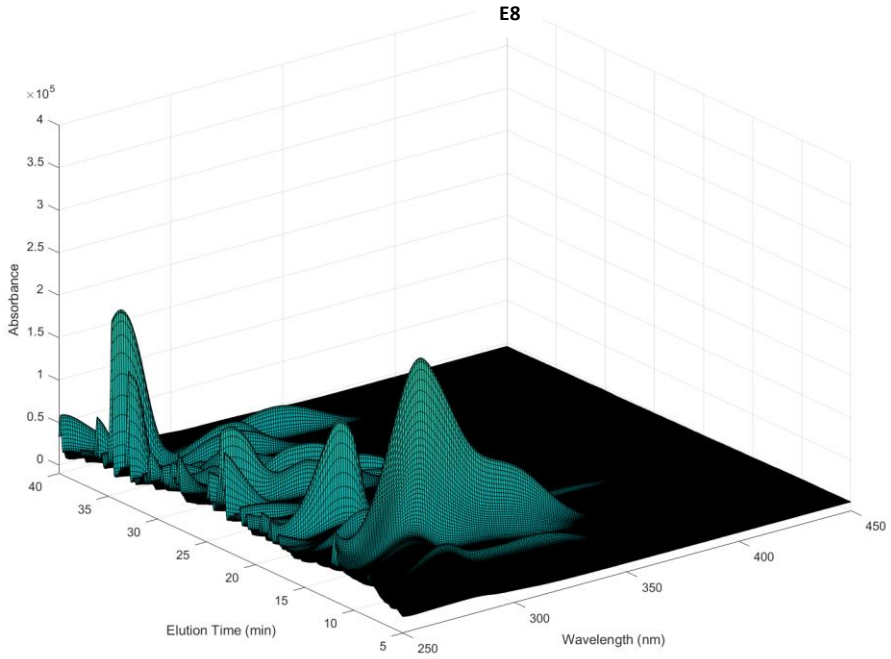

Figure 18: 3D HPLC-DAD chromatogram for the bark of Pinus pinaster tree extract obtained according to the conditions in table 5.

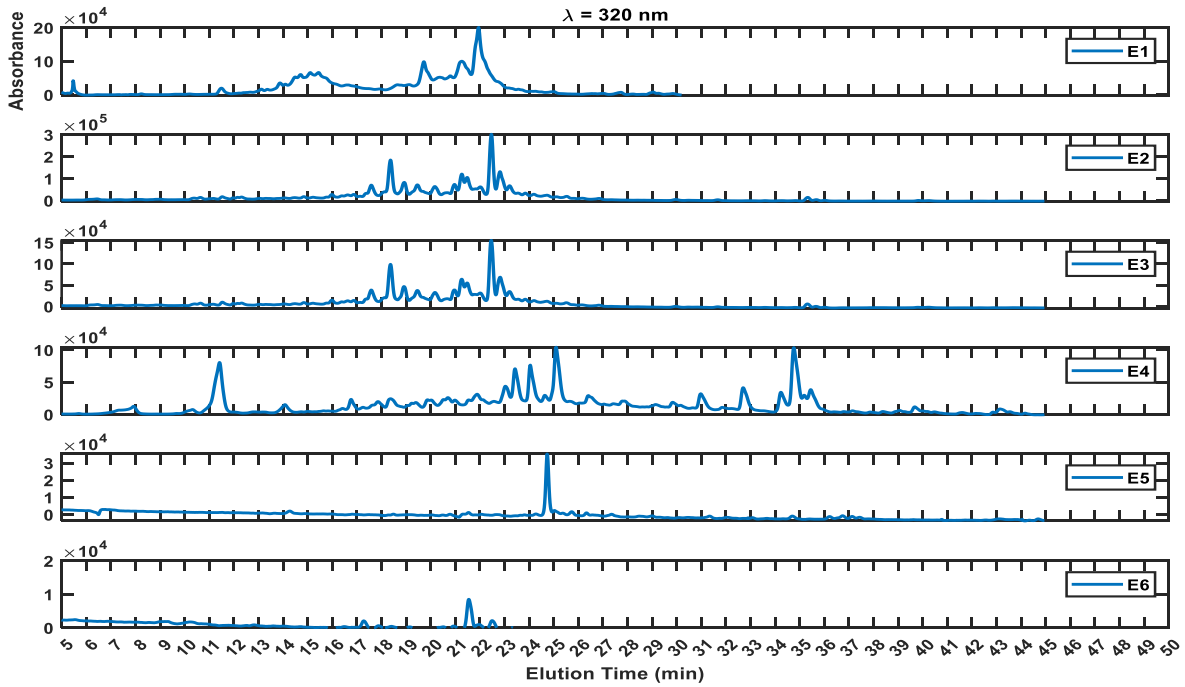

-

Figure 19:: Comparative 2D HPLC-DAD Chromatograms at 320 nm of Phenolic Extracts from Different Parts of Pinus pinea and Pinus pinaster.

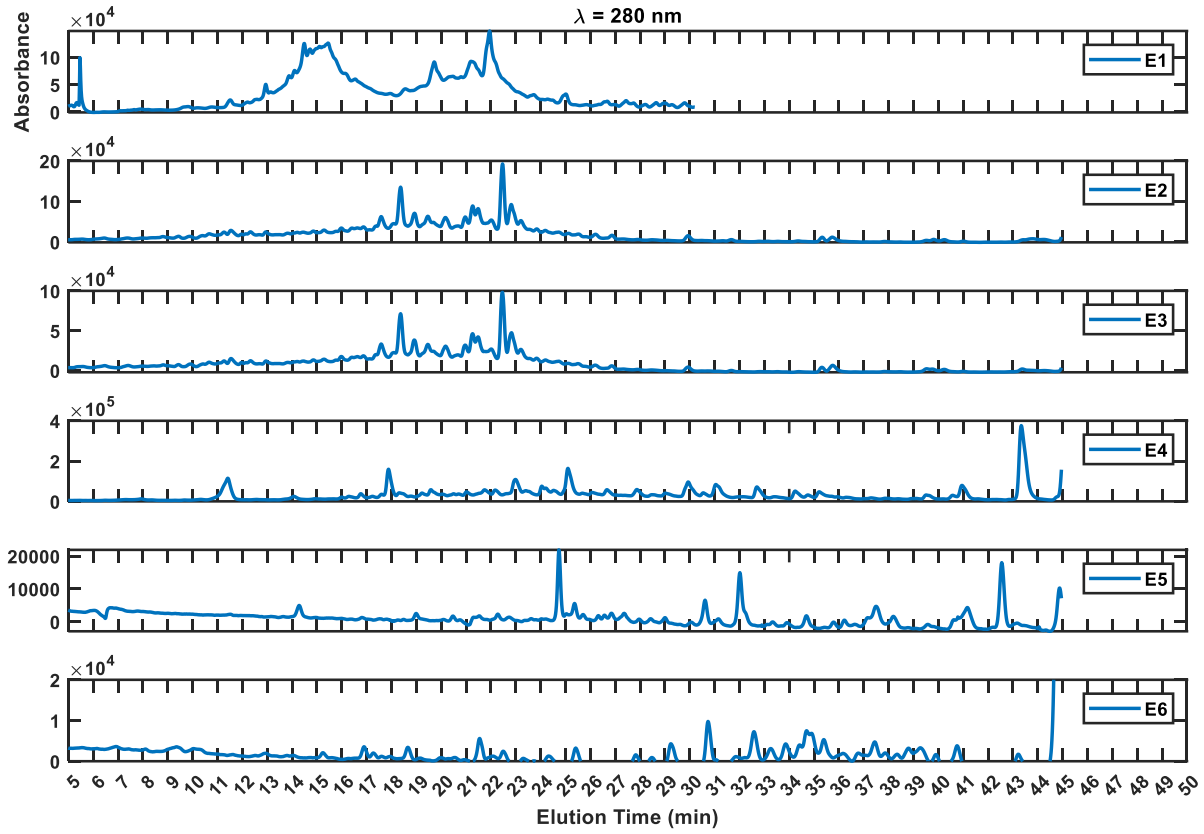

Figure 20: Comparative 2D HPLC-DAD Chromatograms at 280 nm of Phenolic Extracts from Different Parts of Pinus pinea and Pinus pinaster

The comparative analysis of the 2D chromatograms at wavelengths of λ = 320 nm and 280 nm (Figures 20 and 21) reveals that the analytical method plays a crucial role in the resolution and separation of phenolic compounds. The linear method consistently outperforms the NATAC method by producing clearer and more distinct peaks, as observed particularly in extract E1, where the NATAC method demonstrated lower efficiency in peak separation. Regarding the tree species, extracts from Pinus pinaster (notably E4) generally exhibited more complex and intense phenolic profiles than those from Pinus pinea, indicating a higher concentration or diversity of phenolics in Pinus pinaster. As for the plant parts, bark extracts (E3 and E4) displayed richer and more complex chromatographic profiles compared to those from needles or branches, suggesting that bark is a more phenol-rich tissue. When comparing the solvents, acetonitrile (ACN) was more effective than the ethanol/water mixture (80:20) in extracting phenolic compounds, as evidenced by the higher absorbance and peak density in E4 compared to E3, which were both derived from bark but used different solvents. Finally, the wavelength also influenced the visibility and intensity of phenolic signals; while both λ = 320 nm and 280

nm confirmed the same general patterns, specific compounds responded differently at each wavelength, with some peaks appearing more prominent or better separated at one wavelength than the other, highlighting the importance of using multiple wavelengths for comprehensive phenolic profiling.

4.3 Identification of E4 Compounds Using UV Spectral Analysis:

Figures 21 and 22 display the 2D HPLC-DAD Chromatograms recorded at λ = 320 nm and λ = 280 nm, respectively, for extract E4 obtained from the bark of Pinus pinaster. In both chromatograms, several well-defined peaks were detected, five at 320 nm and seven at 280 nm, each presumed to correspond to a different compound. To elucidate the identity of these compounds and explore their chemical classification, UV absorption spectra were compared to reference standards. At 280 nm, the analysis focused on potential lignan compounds by comparing the spectral profiles with those of pinoresinol, secoisolariciresinol, and sesamol (Figure 23). At 320 nm, the aim was to identify possible stilbenes derivatives by comparing the observed spectra to that of resveratrol, a well-established stilbene standard (Figure 24). These comparisons allowed for a preliminary identification of certain peaks as belonging to the lignan or stilbene classes, based on spectral similarities and chromatographic behavior

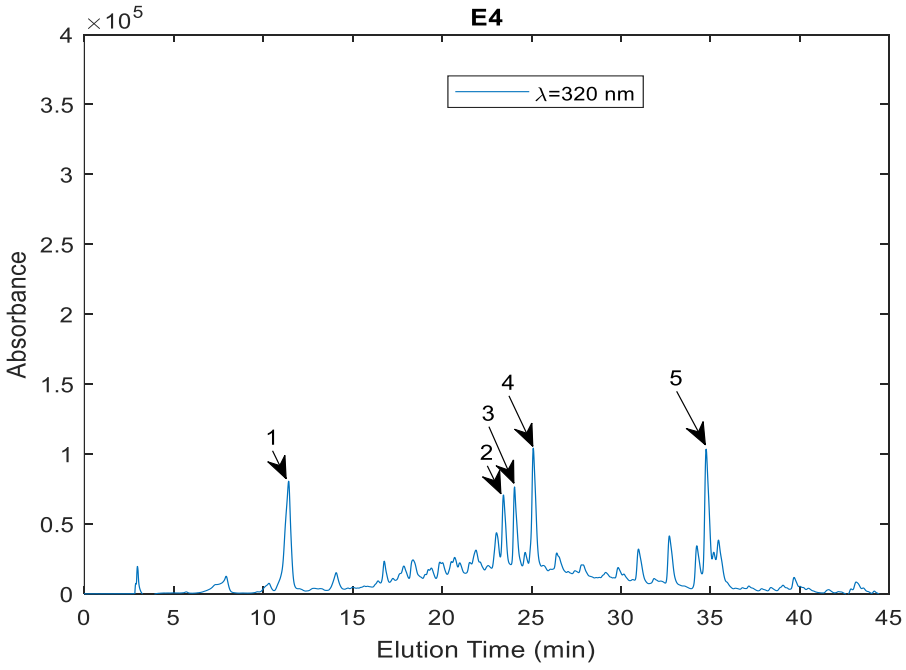

Figure 21: 2D HPLC-DAD chromatogram measured at λ=320 nm for the bark of Pinus pinaster tree extract E4.

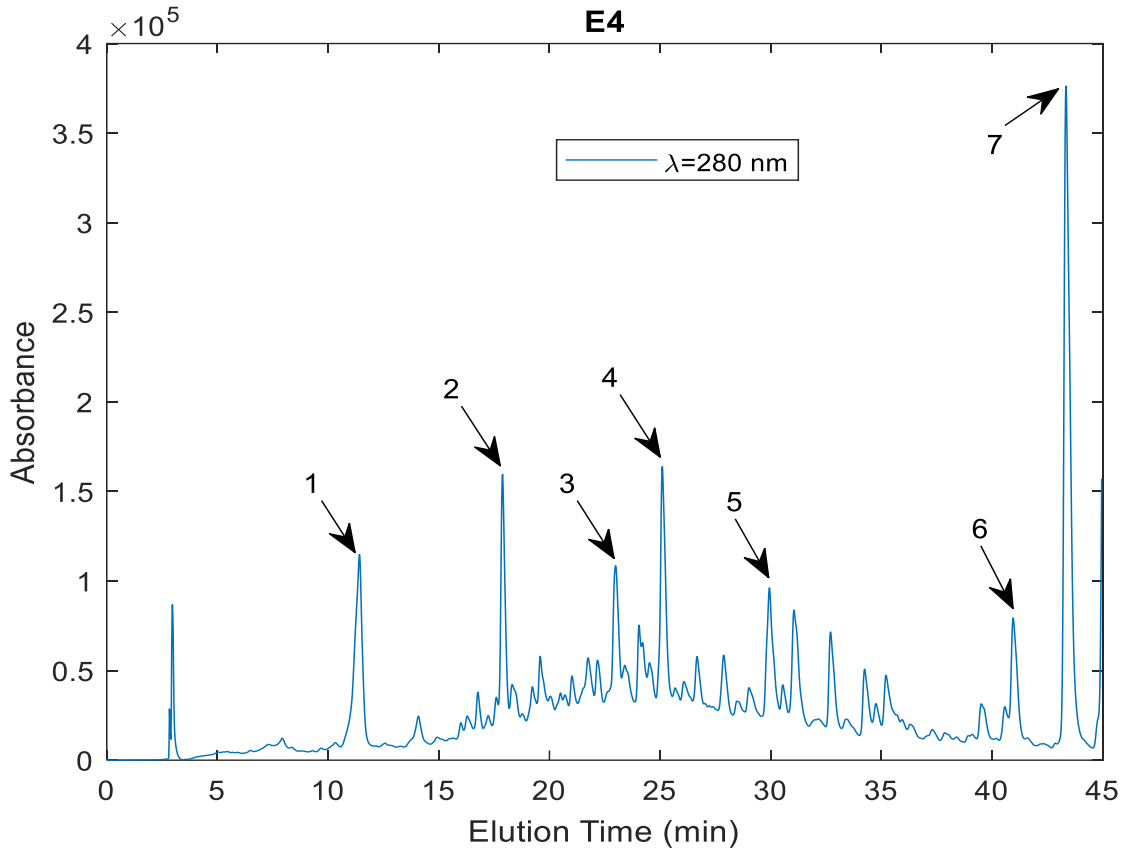

Figure 22: 2D HPLC-DAD chromatogram measured at λ=280 nm for the bark of Pinus pinaster tree extract E4.

a)

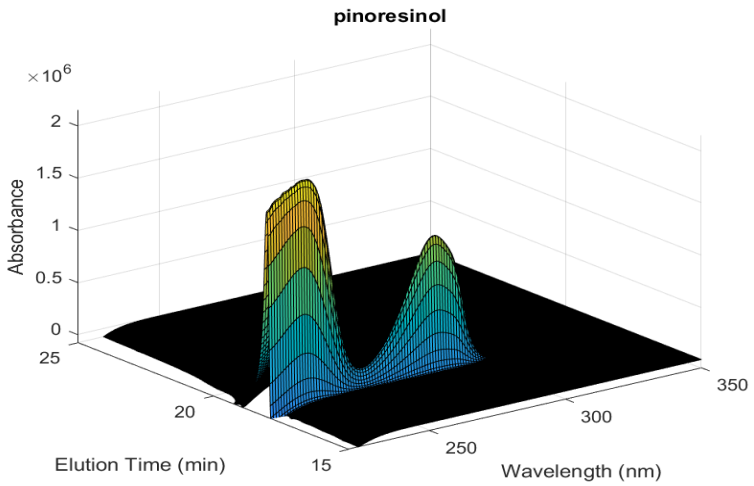

b)

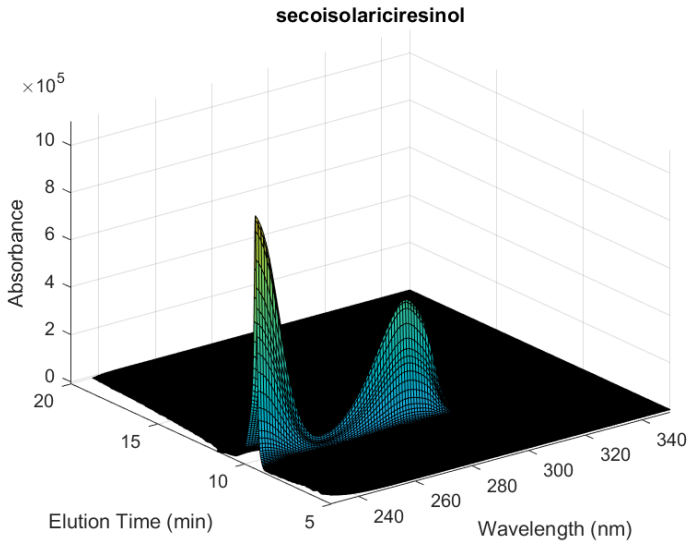

c)

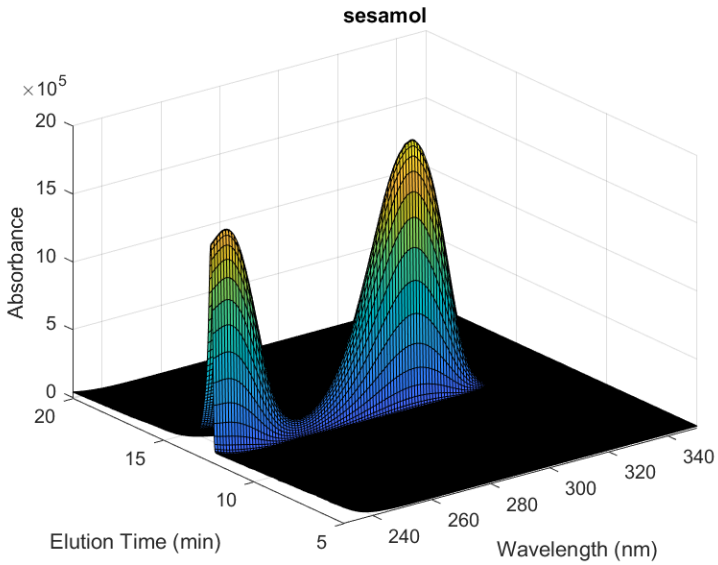

Figure 23: HPLC-DAD chromatograms for lignan standards: a) pinoresinol, b) secoisolariciresinol, and c) sesamol.

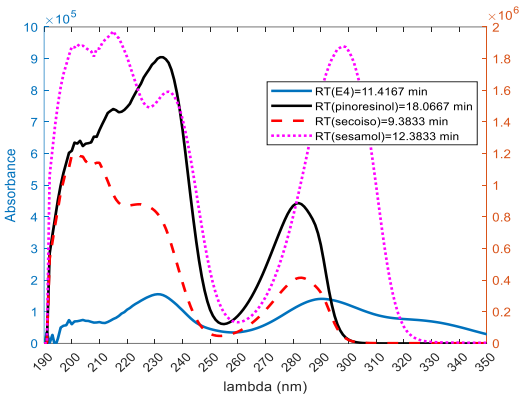

Peak 1

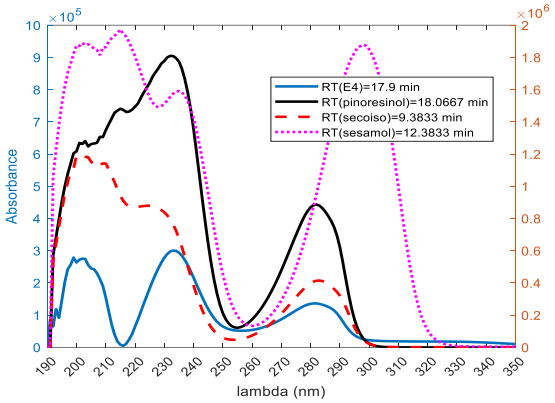

Peak 2

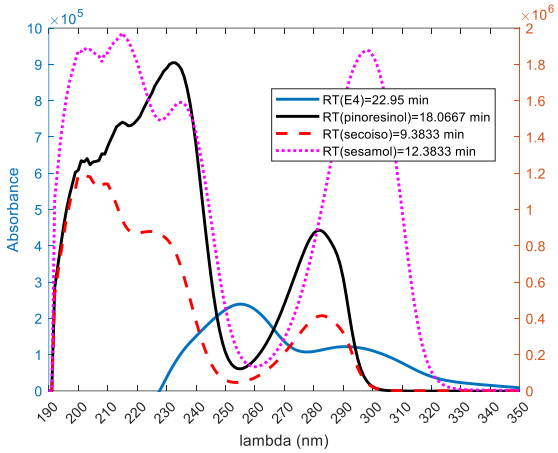

Peak 3

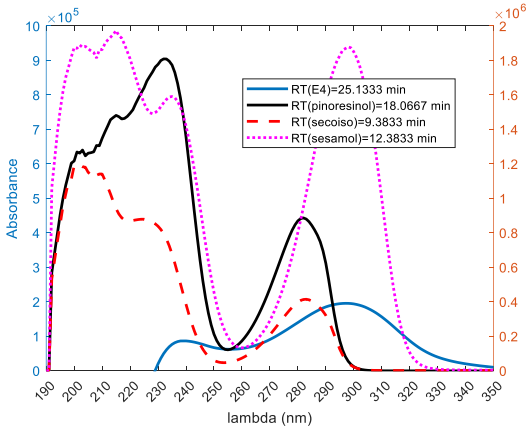

Peak 4

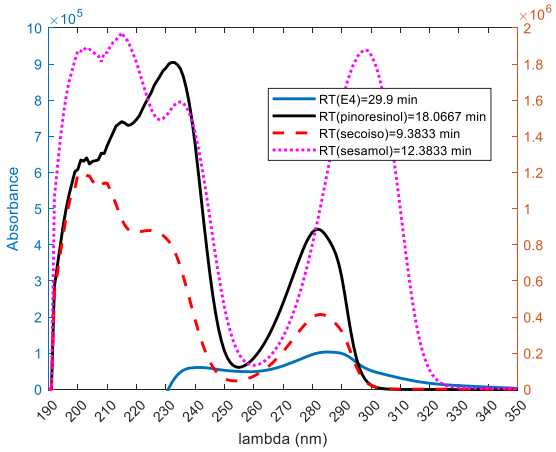

Peak 5

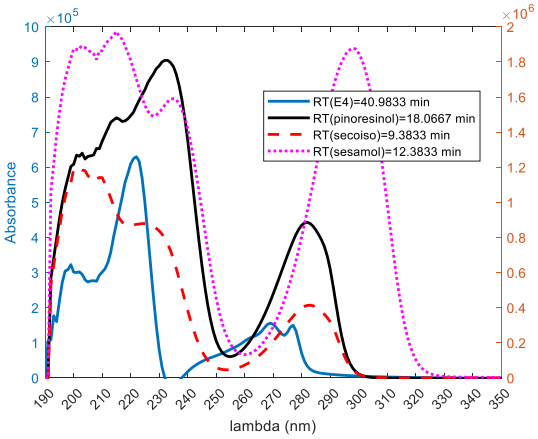

Peak 6

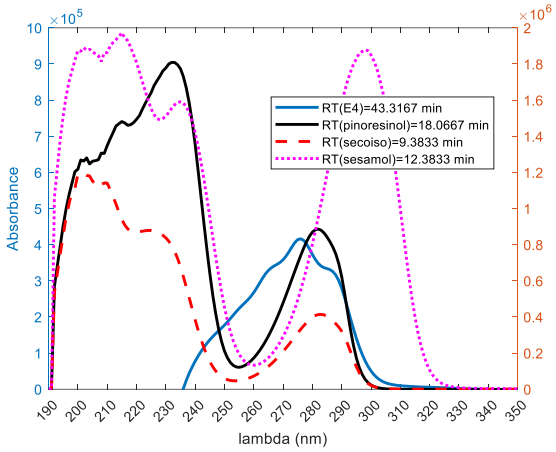

Figure 24: Spectral comparison between 7 peaks of E4 at λ=280 nm and standards: pinoresinol, secoisolariciresinol, and sesamol.

All lignans exhibit a characteristic UV absorption pattern typical of aromatic compounds, with three bands in the regions of 210, 230, and 280 nm. The absorbance of lignans typically decreases in the order: 210 > 230 > 280 nm [28]. This pattern is observed in the reference compounds pinoresinol and secoisolariciresinol; however, it does not apply to sesamol, which is classified as a neolignans rather than a fundamental lignan. Based on spectral comparison (figure 24), peaks 1, 2, and 6 exhibited a UV absorption spectrum consistent with the characteristic spectral profile of lignans, marked by three distinct absorption bands at approximately 210, 230, and 280 nm, suggesting that this compound may belong to the lignan class. Peak 5 presented a spectrum characterized by a waviness and extended tail beyond 240 nm, suggesting the presence of a closed furan ring and a repeated phenolic pattern. These peaks are strong candidates for being pinoresinol or structurally related derivatives. The absence of absorption at 280 nm in Peaks 3 and 4 suggests that these peaks may correspond to non-lignan compounds. However, peak 7 displays a pronounced absorption within the 270-280 nm range, a spectral feature typically associated with lignan- type compounds, thereby suggesting its potential classification within this group.

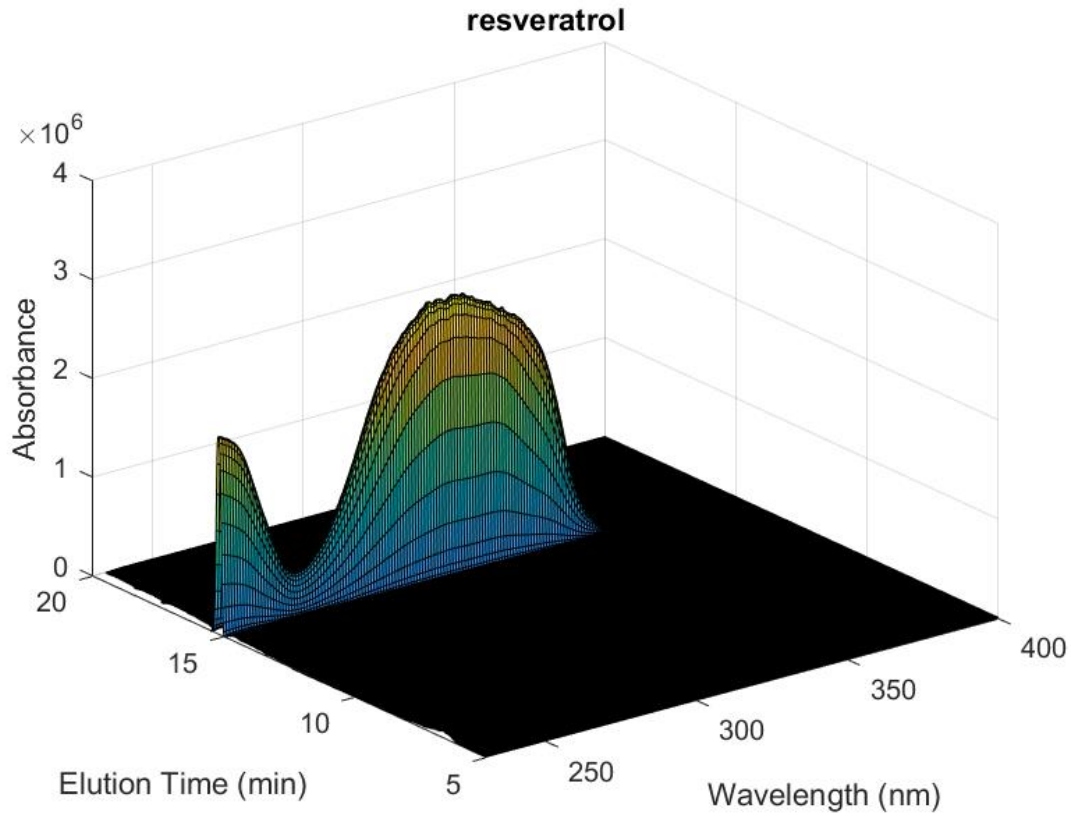

Figure 25: HPLC-DAD chromatograms for resveratrol.

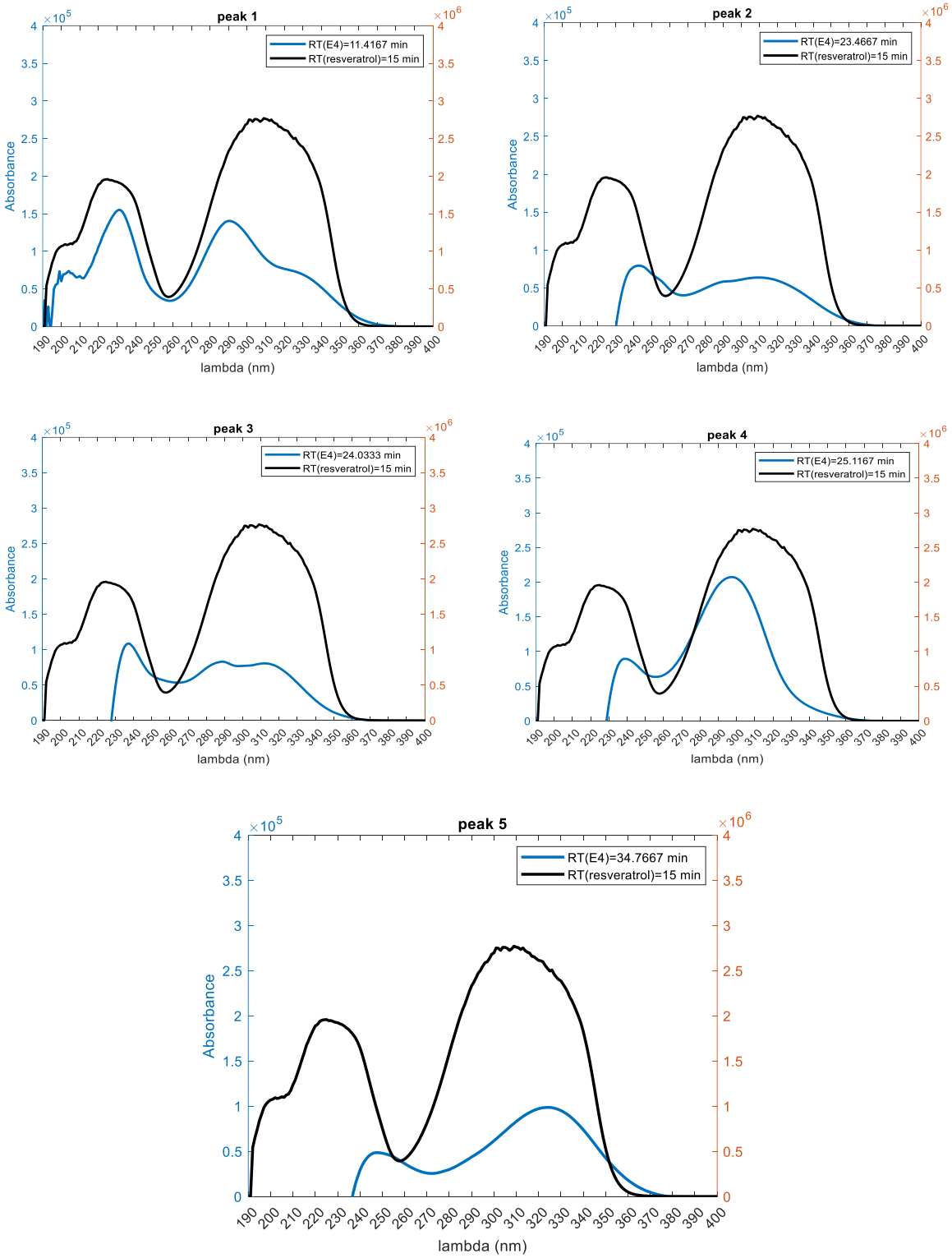

Figure 26: Spectral comparison between 5 peaks of E4 at λ=280 nm and resveratrol.

The UV absorption spectra of the five isolated compounds (Figure 26) were compared to that of a resveratrol standard (black curve), a well-known reference compound from the stilbene family. In graphs 1, 2, and 5, the blue spectra display a high degree of similarity with the

resveratrol profile, both in terms of band position and shape, suggesting the presence of a conjugated aromatic system consistent with typical stilbenes. These similarities support the classification of these compounds within the stilbene family. In contrast, graphs 3 and 4 reveal clear differences, particularly a weakened or absent absorption band around 300 nm. This divergence suggests either a disruption of the conjugated system or a structural modification, indicating that these compounds are less likely to be classical stilbenes. Overall, the UV spectral comparison highlights the ability to distinguish between stilbene-type compounds and those with differing aromatic frameworks based on their absorption profiles.

4.4 Adsorption-Desorption Performance of Polymer Network Toward Extract E4

4.4.1 Adsorption Performance of Polymer Network

The extract prepared from the bark of Pinus Pinaster E4 was used with the prototype illustrated in figure 7 to highlight the efficacy of the synthesized Polymer Network adsorbent with the fractionation of the target classes of molecules. For that purpose, initially, the material was loaded with E4 extract at T = 20°C with a flow rate of 1 mL/min, for 24h, considering a recycling mechanism, the solvent considered was ACN. To ensure the stability and efficiency of the 24-hour adsorption process, pressure was continuously monitored. The consistent profile confirms that the system remained stable throughout the experiment. The efficiency of the adsorption process was assessed by analyzing the final extract using HPLC and comparing the result with that of the original E4 extract prior to adsorption. Figure 28 shows that the blue curve, representing the extract after the adsorption process, shows a clear decrease in most peaks compared to the orange curve, which represents the extract before adsorption particularly in the range between 10 and 35. This indicates that the Polymer Network material successfully adsorbed a significant portion of the compounds present in the extract, especially those corresponding to these peaks. However, some peaks did not completely disappear, suggesting that the adsorption was not total or that some compounds had low affinity for the binding sites on the Polymer Network. It is likely that compounds with stronger absorbance, such as certain lignans, were retained more efficiently. The noticeable difference between the two curves highlights the ability of Polymer Network to selectively adsorb phenolic compounds, including lignans. The reduction of UV peaks after passing through the Polymer Network material serves as strong evidence of the interaction between these compounds and the adsorbent. Therefore, this analysis clearly demonstrates the effectiveness of Polymer Network in capturing phenolic

compounds from the E4 extract, making it promising option for the purification of plant extracts containing bioactive compounds such as lignans.

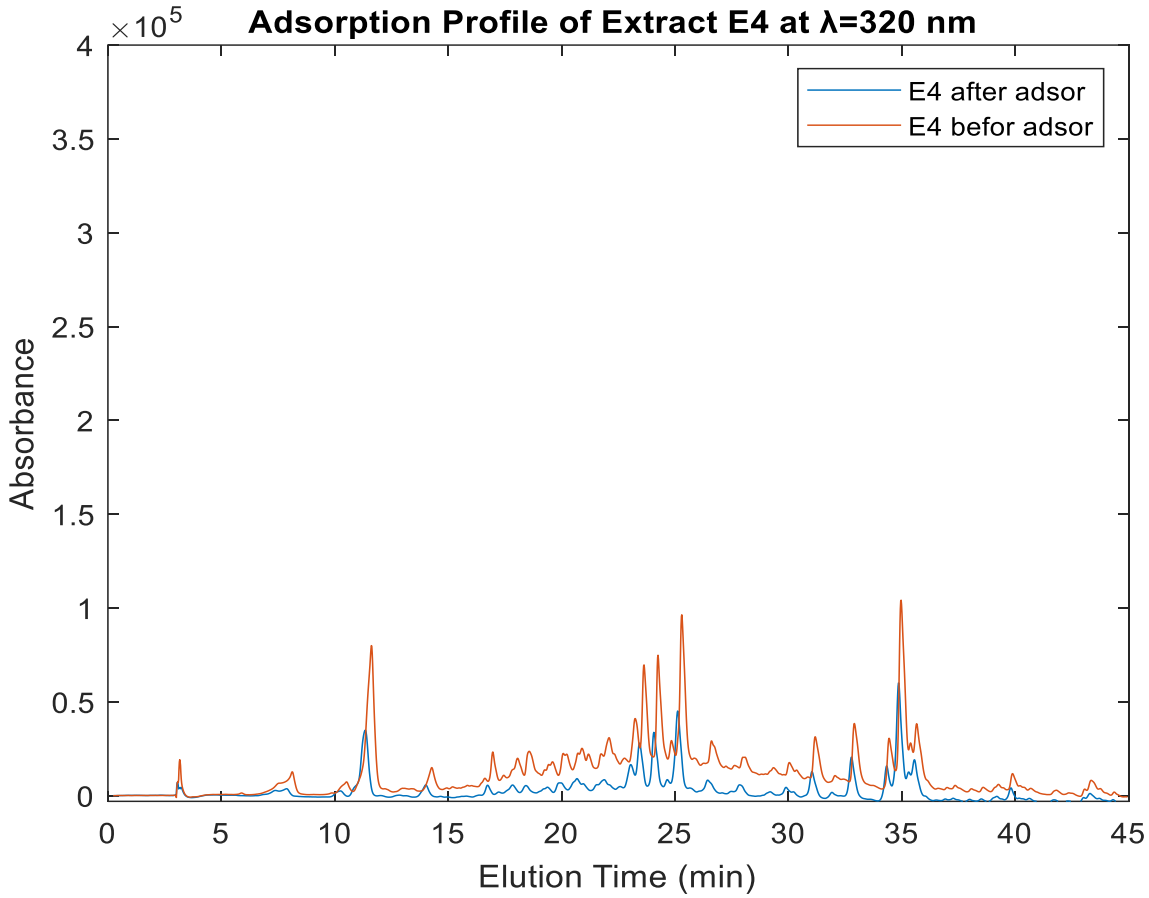

Figure 27: HPLC chromatograms acquired at 320 nm to compare E4 before adsorption with E4 after adsorption.

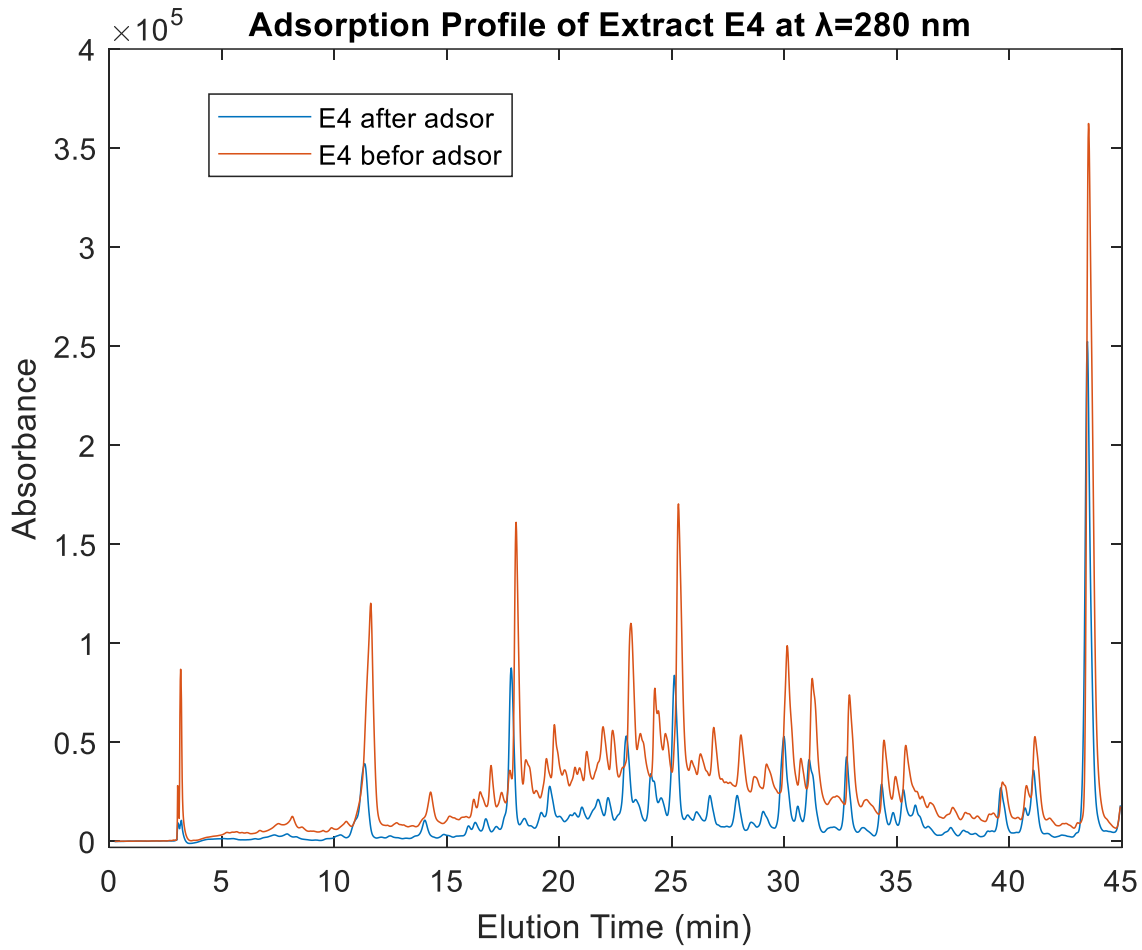

Figure 28: HPLC chromatograms acquired at 280 nm to compare E4 before adsorption with E4 after adsorption.

4.4.2 Desorption Performance of Polymer Network

After the extract loading step in the Polymer Network particles, the fractionation (elution) process was carried out at T= 45 °C. The subsequent stage involved the use of ten distinct elution solvents, which included pure water, mixtures of ethanol/water, pure ethanol, pure methanol (MeOH) and pure ACN. Table 6 presents the solvents used and the corresponding compositions for each elution fraction. Figures 29 and 30 show the HPLC-DAD 2D chromatograms of the *Pinus pinaster* bark extract in ACN, used for loading the polymer network particles, along with the corresponding fractions collected after elution with the different solvents described in Table 6. Measurements at 280 nm highlighted the separation and purification of lignans, while those at 320 nm revealed the behavior of stilbenes.

Table 6: Solvent and their compositions used in each elution fraction

Fractions	Solvent	Composition(V/V)
F0	Water	100
F1	Ethanol/Water	40/60
F2	Ethanol/Water	50/50
F3	Ethanol/Water	60/40
F4	Ethanol/Water	70/30
F5	Ethanol/Water	80/20
F6	Ethanol/Water	90/10
F7	Ethanol	100
F8	MeOH	100
F9	ACN	100

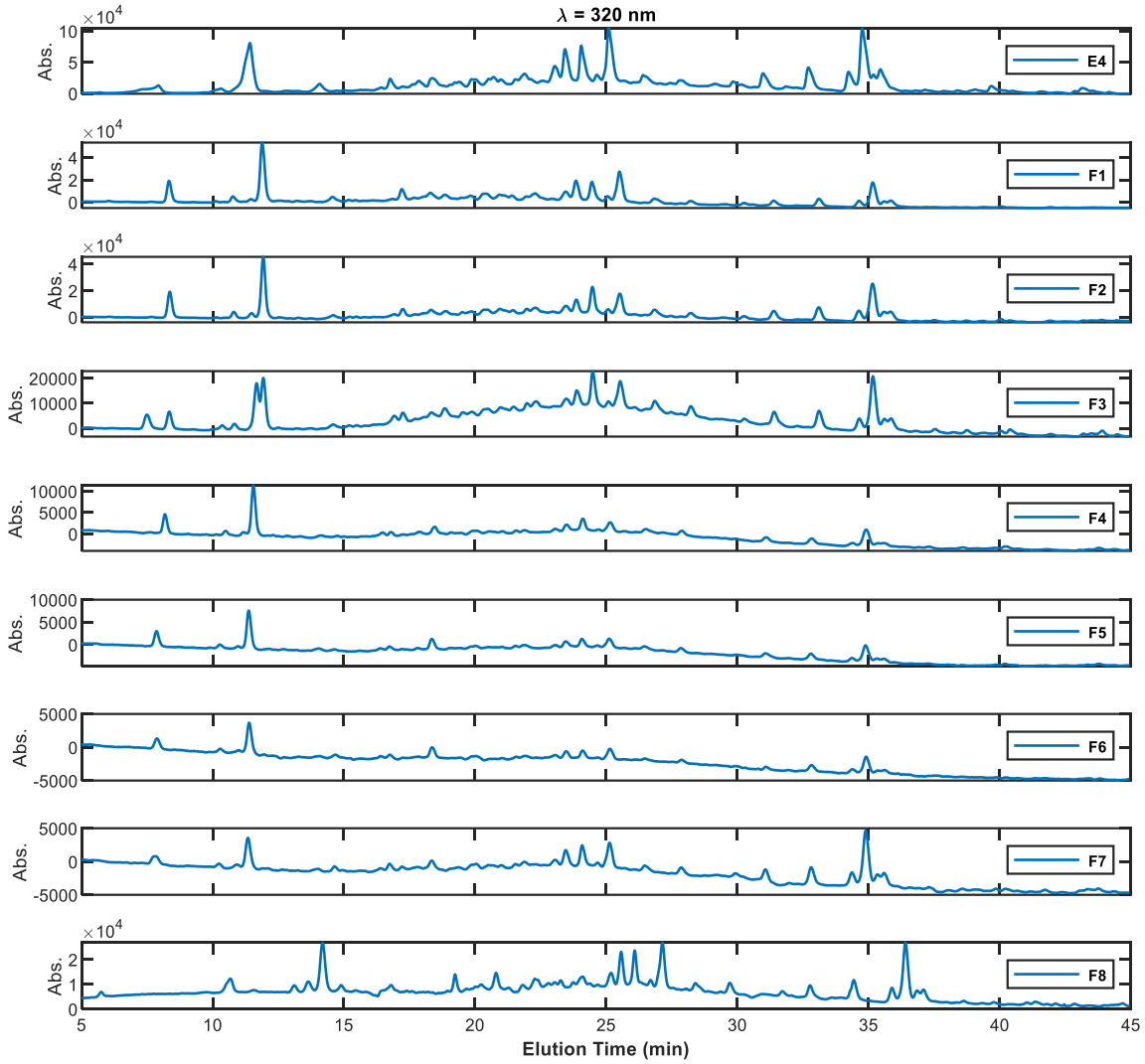

Figure 29: 2D HPLC-DAD chromatograms for the initial extract E4 and for fractions collected during the desorption process of the compounds retained in the Polymer Network adsorbent.

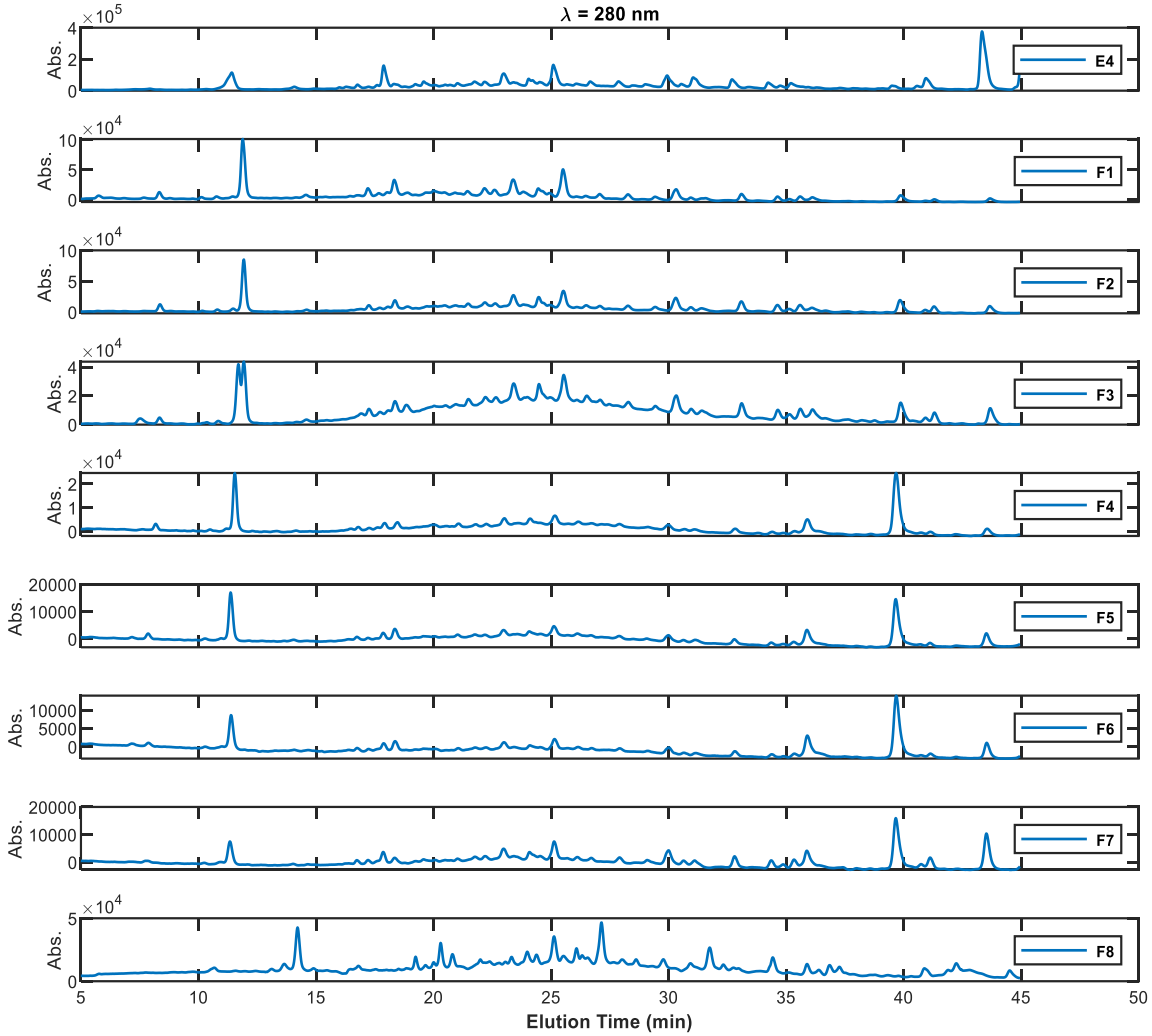

Figure 30: 2D HPLC-DAD chromatograms for fractions collected during the desorption process of the compounds retained in the Polymer Network adsorbent.

The results indicate that the fractions obtained after the elution process did not exhibit a clear simplification in composition compared to the initial extract (E4). Instead, they retained most of the same compounds but at lower concentrations. This suggests that the polymer network material failed to achieve an effective selective separation of phenolic compounds and merely reduced their concentrations without significantly altering their compositional diversity.

To accurately assess the inefficiency of the Polymer Network material in achieving selective separation, a 2D HPLC-DAD chromatogram was conducted for both the crude extract E4 and the fractions obtained after the elution process (F6, F5, and F4, etc.) at 280 nm. In each chromatogram, the seven most intense peaks were selected, as they represent the most abundant

compounds in each sample. The area of each peak was then calculated as a percentage of the total area of the selected peaks, allowing for an estimation of the relative distribution of compounds within each sample. These data were compiled and summarized in Table 7 to facilitate the comparison of percentage values in each fraction with those recorded in the E4 extract. This comparison aimed to evaluate whether the Polymer Network material altered the chemical fingerprint of the extract by selectively removing specific compounds, or if it simply acted as non-specific adsorbent that reduced overall concentration without affecting compound diversity.

Table 7: Relative Peak Area Distribution of the Eight Most Intense Compounds in Crude Extract E4 and Eluted Fractions Based on 2D-HPLC Analysis at λ=280 nm.

N° of peak	**1**	**2**	**3**	**4**	**5**	**6**	**7**
Area (%) E4	5.1	0.7	4	4.3	7.1	3.2	4
Area (%) F1	4.8	2	2.7	3.1	4.8	1.7	3.2
Area (%) F2	3.4	1.3	2	3.2	3	2.5	3.9
Area (%) F3	1.5	1.2	2.2	3.6	3.3	2.9	3.4
Area (%) F4	2.8	_	_	2.7	1.3	0.8	0.6
Area (%) F5	4.6	0.984	_	1.4	2.2	0.4	1.2
Area (%) F6	3.3	1.1	1.9	2	3.8	0.5	0.9
Area (%) F7	0.9	0.5	1.8	3.2	3.6	2.9	4.5

The results in table 7 showed that most peaks were retained across various fractions, but at lower percentages compared to the original extract. For instance, peak 1 gradually decreased from 5.1% in E4 to 0.9% in the ethanol fraction, a pattern observed for most other peaks, such as Peaks 3, 4, 5, and 6. Notably, peak 2 showed an unexpected increase in F6 (2%) compared to E4 (0.7%), reflecting irregular, non-selective behavior. Peak 7 displayed relatively stable levels across some fractions, yet their final decrease supports the overall trend of concentration reduction without a simplification in chemical composition. Based on these observations, it is evident that the polymer network material acted as a non-selective adsorbent, reducing the concentrations of phenolic compounds without achieving an effective selective separation.

4.5 Adsorption-Desorption Performance of Polymer Network Toward Extract E7

4.5.1 Adsorption Performance of Polymer Network

HPLC chromatograms recorded at wavelength of 280 nm (Figure 31) clearly demonstrate a comparative analysis of extract E7 before adsorption and after adsorption using the poly(2,6-bis(acrylamido)pyridine) polymer network. The extract E7 before adsorption reveals the presence of bioactive compounds, as indicated by the sharp and prominent peaks, particularly in the retention time regions around 3 and 13 minutes, suggesting a high concentration of phenolic or aromatic compounds in the crude extract. Following treatment with the polymer, some peaks showed a significant decrease while others remained almost unchanged. These results highlight the effectiveness of the poly(2,6-bis(acrylamido)pyridine) network in adsorption processes.

To accurately interpret the adsorption results of pinoresinol for example, it is essential to understand their interactions with the polymer network of poly(BAAPy). Figure 32 illustrates proposed interaction models between pinoresinol and poly(BAAPy). The pinoresinol molecule can strongly bind to the polymer through several non-covalent interactions that enhance adsorption efficiency. The most important of these interactions are hydrogen bonds, where the hydroxyl (–OH) groups in pinoresinol can bind to the oxygen atoms in carbonyl (C=O) groups or to nitrogen atom in the pyridine ring within the polymer. The methoxy group ($–OCH_3$) can also participate in hydrogen bonding with hydrogen-donor N–H groups in polymer. In addition, the furofuran ring in pinoresinol contains two oxygen atoms that can act as hydrogen acceptors from N–H groups in polymer, adding extra binding sites that strengthen the interaction. Furthermore, due to the cyclic nature and the lone-pair electron on oxygen, this part of the molecule may contribute to compound stability through electrostatic interactions or aid in molecular arrangement via steric effects. π–π stacking interactions between the aromatic rings of both molecules, as well as N–H···π interactions, further enhance the stability of the resulting complex, granting the polymer high selectivity and efficiency in retaining pinoresinol.

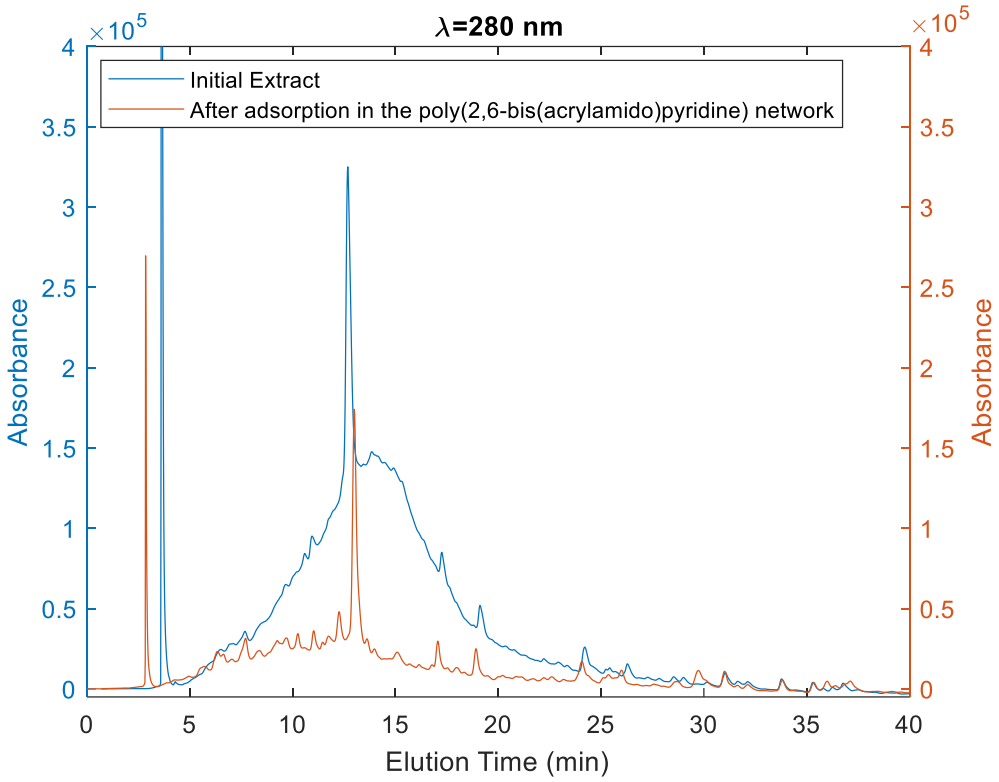

Figure 31: HPLC chromatograms acquired at 280 nm to compare E7 before adsorption with E7 after adsorption.

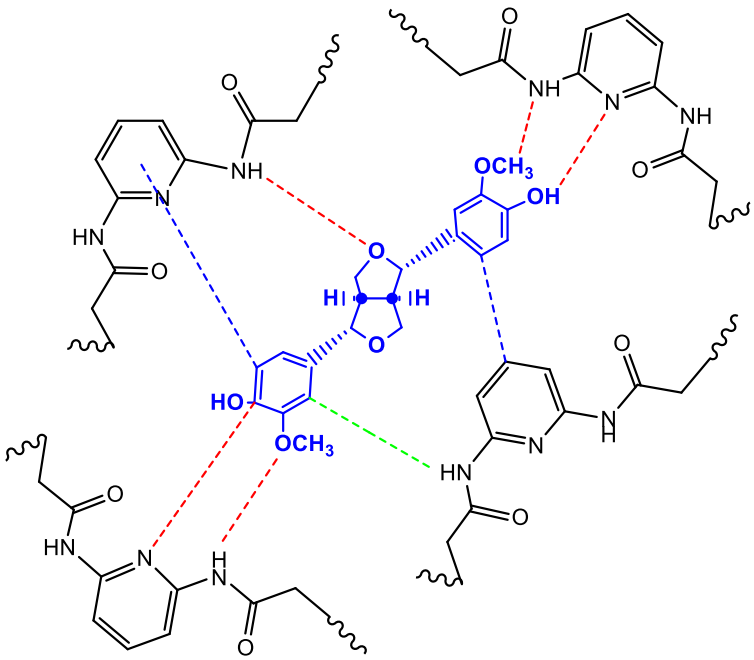

Figure 32: Illustration of proposed non-covalent interactions between poly (BAAPy) and pinoresinol identified in the pinus These structures represent plausible interaction models based on established non-covalent binding principles. Hydrogen bonding (red), amide

4.5.2 Desorption Performance of Polymer Network

The three figures (33, 34 and 35) display high-performance liquid chromatography (HPLC) chromatograms acquired at 280 nm, aimed at evaluating the desorption efficiency of phenolic compounds from a plant extract using the polymeric network poly(2,6-bis(acrylamido)pyridine) with different hydroalcoholic mixtures. The first figure (Figure 33) represents a blank injection, which refers to an analysis performed without any sample. It shows minor peaks between 20 and 40 minutes, which are attributed to the system not to any components of the extract. Therefore, these peaks must be disregarded in the actual interpretation of desorption performance.

The second figure (Figure 34) compares the initial extract with fractions desorbed from the polymer using six different water/ethanol or methanol/acetone mixtures. The third figure (Figure 35) compares the initial extract with a concentrated desorbed fraction obtained using a 60/40 water/ethanol mixture.

The analyses reveal the presence of two main peaks at retention times of 13.5 and 18.7 minutes. The peak at 13.5 minutes is identified as corresponding to a pinoresinol-related compound (probably a pinoresinol glucoside or diglucoside) [72] [73], while the peak at 18.7 minutes corresponds to pinoresinol (see Figure 36). The results indicate that the water/ethanol mixtures at ratios of 60/40 and 40/60 offer the best efficiency in the removal of pinoresinol (see Figures 34 and 35). This can be inferred from the concentration of the eluted fraction using the 60/40 mixture (see Figure 35), as the results showed a significant increase in the intensity of the peak at 18.7 minutes, clearly indicating an improvement in the recovery of pinoresinol and an increase in its concentration in the sample.

In conclusion, the polymer poly(2,6-bis(acrylamido)pyridine) demonstrates high efficiency in selectively adsorbing phenolic compounds from plant extracts, especially when using a 60/40 water/ethanol mixture. Moreover, the concentration step effectively enhances separation performance and facilitates the recovery of key bioactive molecules such as pinoresinol and pinoresinol glucoside or diglucoside [72] [73].

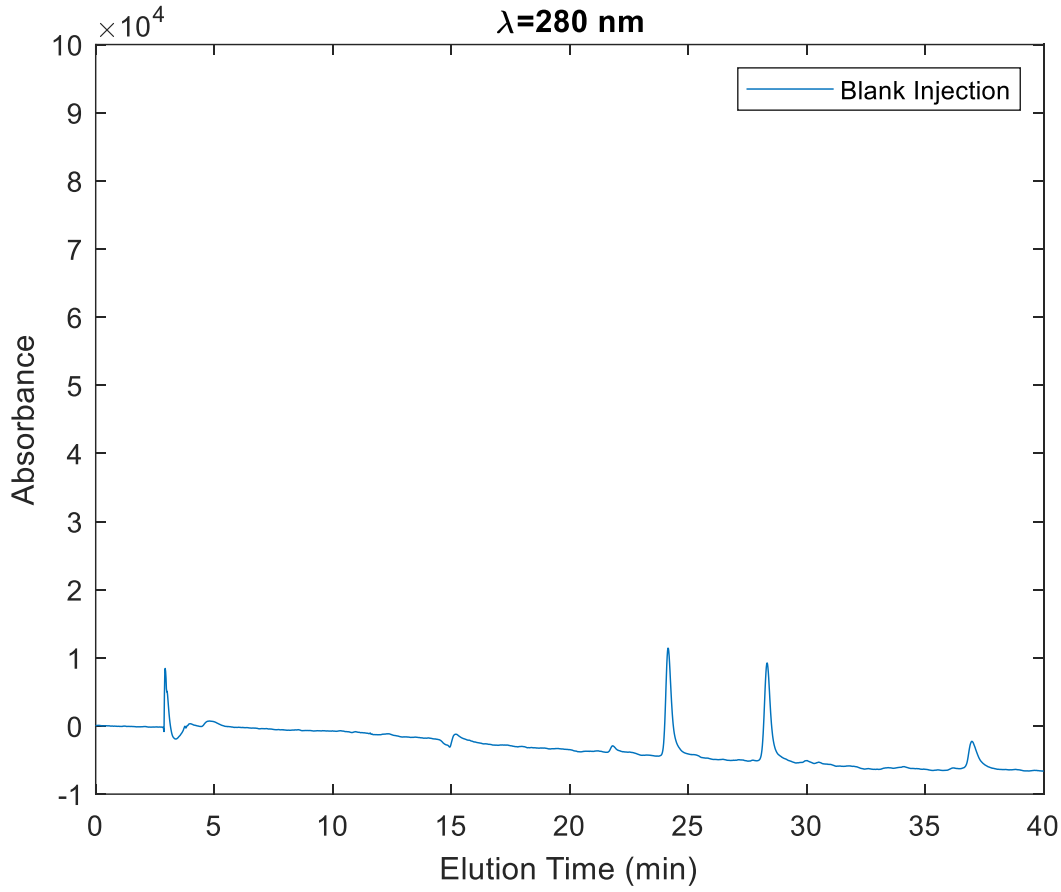

Figure 33: HPLC chromatogram for a blank injection acquired at 280 nm highlighting the system peaks appearing at the region 20 to 40 min that are not part of the extracts or eluted fractions.

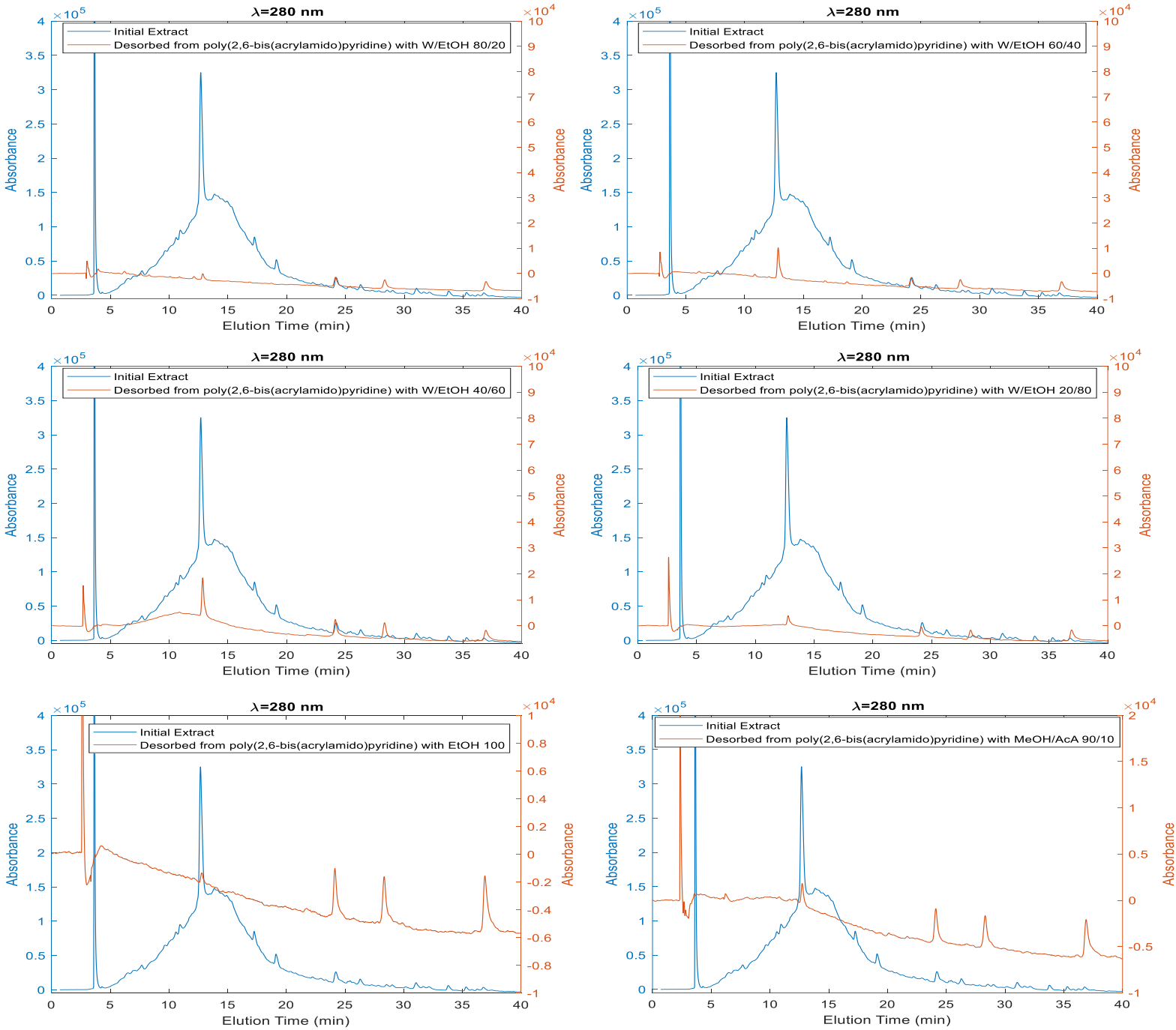

Figure 34: HPLC chromatograms acquired at 280 nm to compare the initial extract and fractions desorbed from the poly(2,6-bis(acrylamido)pyridine) polymer network considering hydroalcoholic mixtures with different compositions.

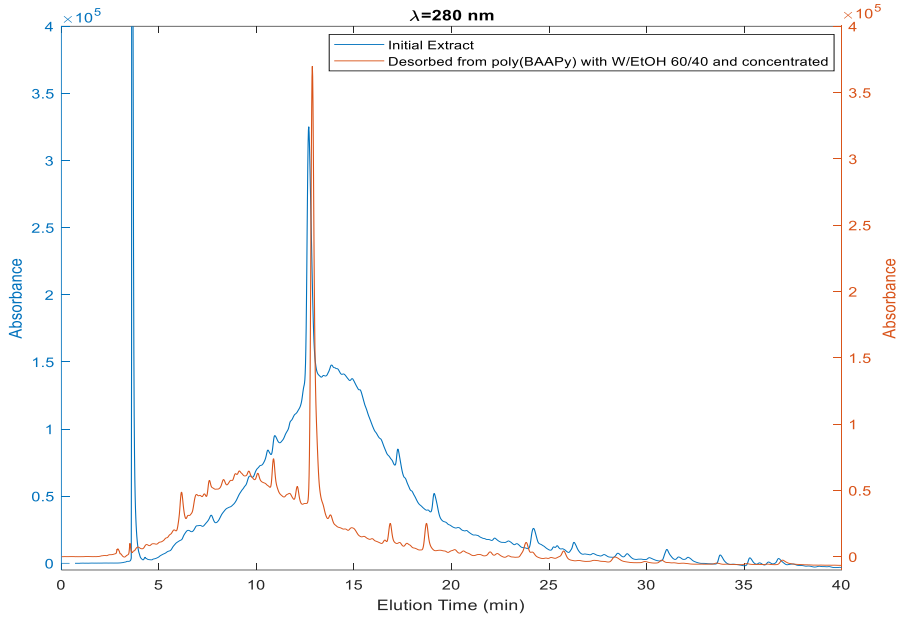

Figure 35: HPLC chromatograms acquired at 280 nm to compare the initial extract and a concentrated fraction desorbed from the poly(2,6-bis(acrylamido) pyridine) polymer network considering hydroalcoholic mixture with composition water/ethanol 60/40.

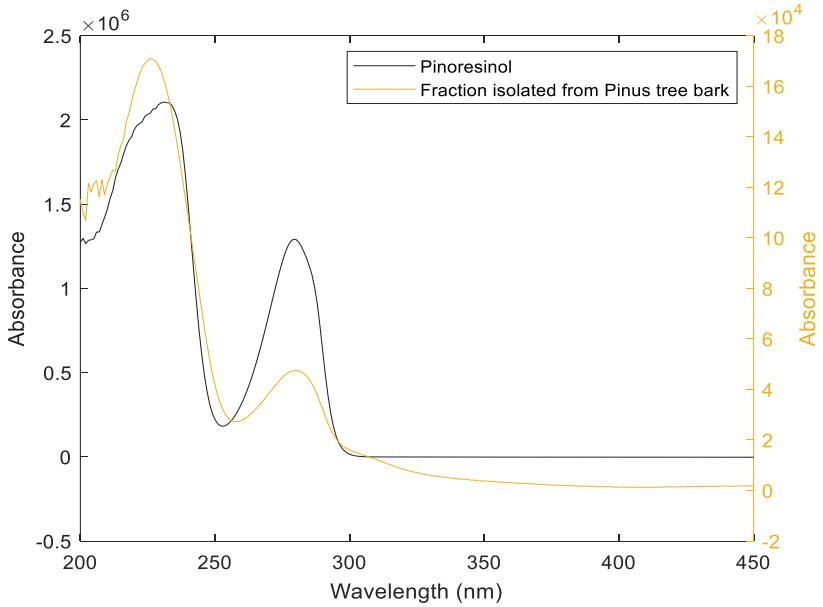

Figure 36: UV spectrum of the pinoresinol standard and the major compound in a fraction isolated from Pinus tree bark through sorption/desorption in the poly(2,6-bis(acrylamido)pyridine) polymer network. This fraction is correspondent desorption with water/eth

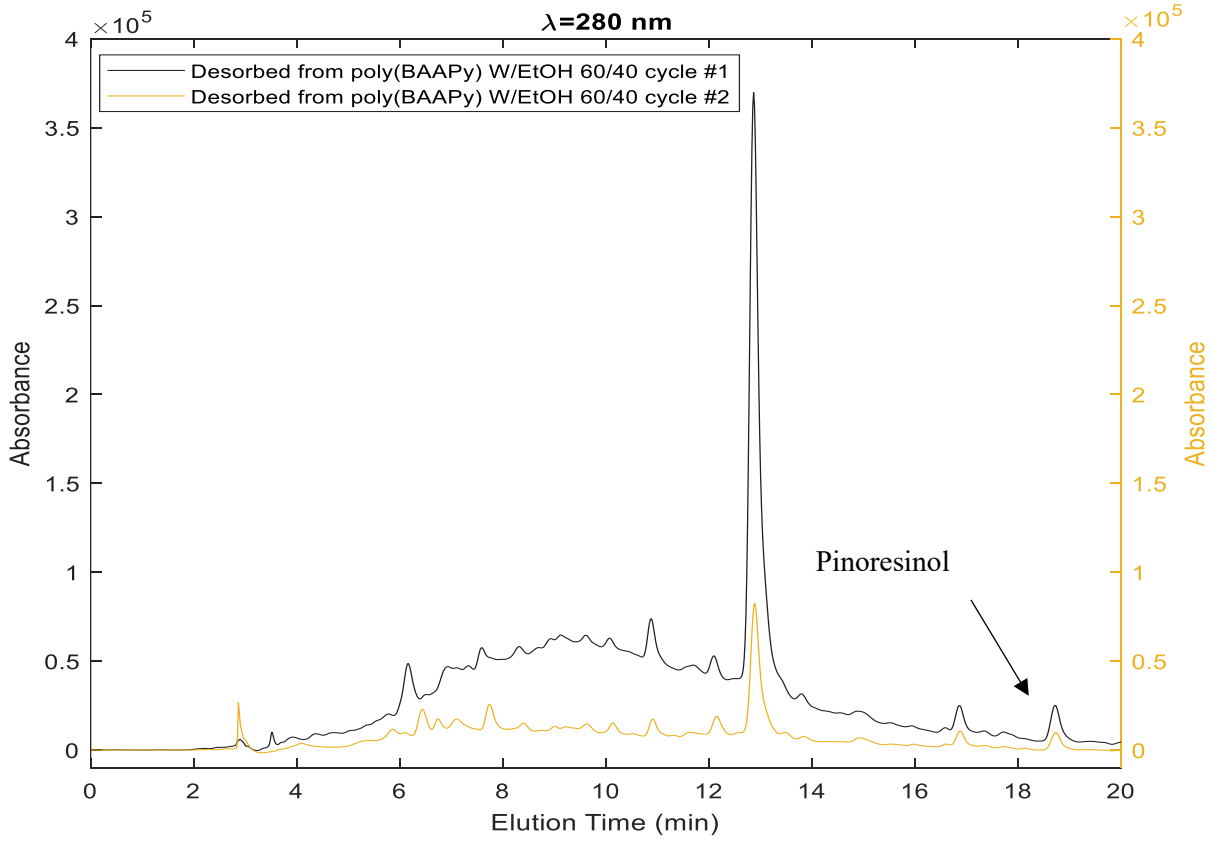

Figure 37: HPLC chromatograms acquired at 280 nm illustrating the multicycle of sorption/desorption with the bis(acrylamido)pyridine) polymer network and the pinus tree bark extract.

Figure 37 presents high-performance liquid chromatography (HPLC) chromatograms recorded at 280 nm, illustrating the adsorption/desorption behavior over two

cycles using the bis(acrylamido)pyridine polymer network with an extract from pine tree bark. The same hydroalcoholic mixture (water/ethanol 60/40) was employed in two consecutive sorption/desorption cycles.

The chromatograms (cycle 1 and cycle 2) clearly demonstrate the high efficiency of the polymer during the first cycle, as indicated by a sharp and intense peak at approximately 13.5 minutes is identified as corresponding to a pinoresinol-related compound (probably a pinoresinol glucoside or diglucoside) [72] [73] , in addition to a significant peak at 18.7 minutes, which has been identified as pinoresinol.

When comparing the first and second adsorption–desorption cycles, a peak corresponding to pinoresinol is still observed at the same retention time, though with slightly lower intensity.

This persistence confirms that the active sites within the polymer network remain functional and structurally stable, indicating good reusability and durability of the material. The observed decrease in intensity is likely due to partial site saturation or minor structural fatigue of the polymer, which may have slightly reduced its adsorption capacity in subsequent uses.

These results suggest that the use of the bis(acrylamido)pyridine polymer with a water/ethanol 60/40 mixture is not only effective for selective adsorption, but also allows for repeated use in multiple cycles, although with a gradual decrease in efficiency. The distinctive peaks at 13.5 and 18.7 minutes confirm the purity of the desorbed fractions and their specificity for lignan compounds, in agreement with previous analyses that showed this mixture offers optimal recovery of pinoresinol.

The repetition of adsorption/desorption cycles in this experiment is not only intended to evaluate the polymer's performance in multiple cycles but also serves as a key indicator of its durability and stability under operational conditions. By monitoring its performance over successive cycles, it is possible to determine whether the polymer can maintain its efficiency after repeated use and preserve the binding sites from damage or loss functionality. Assessing reusability is crucial in industrial applications, as it helps reduce costs and improve economic feasibility, especially if the polymer can be used for ten or twenty cycles without a significant decrease in performance. Furthermore, evaluating long-term performance allows for the early detection of any degradation in the polymer's mechanical or chemical properties, providing valuable data for improving its design and ensuring its effectiveness in large-scale separation and extraction processes. Notably, poly(BAAPy) polymer demonstrated successful performance in this evaluation, which can be attributed to its well-defined three-dimensional network architecture.

The three-dimensional polymer network is of great importance due to the high mechanical strength and durability it provides, thanks to crosslinking points that prevent chain slippage, granting greater thermal and chemical stability compared to linear polymers. While linear polymer may dissolve or soften easily, three-dimensional networks generally do not dissolve but only swell. This structure also allows control over permeability and swelling degree by determining the size of internal pores, a property that is essential in hydrogels and separation material. In the case of separation materials, such as filtration membranes or chromatography columns, the working mechanism relies on the passage and selection of molecules, where the three-dimensional network creates pores of specific sizes that allow certain molecules to pass

while blocking others. This principle is used in the separation of chemical compounds in laboratories and industries. Additionally, this structure enhances the material's resistance to deformation under pressure, making it suitable for applications that require durability and long-term performance.

Chapter 5 General Conclusion

In this work, a robust and sustainable methodology was developed for the selective extraction and enrichment of lignans from pine bark, demonstrating the potential of functional polymer networks in valorizing forestry by-products. Using ultrasound-assisted extraction with an ethanol/water (80:20 v/v) solvent system, a crude pine bark extract rich in phenolic compounds was obtained. A poly(2,6-bis(acrylamido)pyridine) network was synthesized and applied in a pilot-scale sorption/desorption prototype, exploiting the complementary hydrogen-bonding and π–π interactions between the polymer matrix and lignan molecules. Desorption with a water/ethanol (60:40 v/v) mixture afforded fractions highly enriched in lignans, most notably pinoresinol, with an enrichment factor of six relative to the initial crude extract, and a pinoresinol-related compound (probably a pinoresinol glucoside or diglucoside) [72] [73]. The material exhibited excellent stability and reusability, as evidenced by multicycle sorption/desorption experiments that maintained high recovery of target compounds over successive runs.

Despite the successful purification of pinoresinol from extract E7, its chromatogram revealed some limitations. The peak intensity of pinoresinol was lower than in the initial extract, indicating partial loss during the adsorption–desorption process. Additionally, baseline noise and overlapping signals highlighted that the separation was not perfectly selective. These observations suggest that further optimization of the sorption and desorption parameters—such as flow rate, temperature, and solvent composition—is necessary to increase both the yield and purity of the isolated compounds. Another limitation concerns the identification of certain lignans that are likely present in higher amounts in extract E7 but could not be confirmed due to the lack of available reference standards in the HPLC analysis. Incorporating additional lignan reference standards in future HPLC studies would enable more accurate identification and facilitate their targeted purification.

These findings confirm that bis(acrylamido)pyridine-based networks can serve as efficient, selective adsorbents for lignans, combining high capacity with operational simplicity and low solvent consumption. The demonstrated six-fold enrichment underscores the capability of this approach to concentrate bioactive compounds from complex matrices without resorting to extensive chromatographic cascades. Moreover, the successful multicycle operation highlights the polymer’s mechanical and chemical resilience, paving the way for continuous or semi-continuous processing in an industrial context.

Future work should focus on fine-tuning sorption and desorption parameters, such as flow rate, temperature, and solvent composition, to maximize both yield and purity of isolated lignans. Systematic optimization could further enhance selectivity, reduce cycle times, and lower solvent usage. In parallel, the underlying recognition principles can be adapted to other valuable phenolics; in particular, the separation of stilbenes (resveratrol and pinosylvin derivatives) present in Pinus by-products represents an attractive extension. By integrating detailed kinetic and thermodynamic studies, as well as scaling up to pilot-plant volumes, this polymer-based platform holds significant promise for the green, cost-effective production of high-value phytochemicals within a circular-economy framework.

References

[1] R. Chevalier, A. Catapano, R. Pommier, and M. Montemurro, "A review on properties and variability of Pinus Pinaster Ait. ssp. Atlantica existing in the Landes of Gascogne," *Journal of Wood Science*, vol. 70, no. 14, pp. 1–25, Dec. 2024, doi: 10.1186/s10086-024-02127-3.

[2] B. Holmbom *et al.*, "Knots in trees - A new rich source of lignans," *Phytochemistry Reviews*, vol. 2, no. 3, pp. 331–340, Jan. 2003, doi: 10.1023/B:PHYT.0000045493.95074.a8.

[3] Celhay, F., and Clément, A., *"Fractionation of by-products from maritime pine (Pinus pinaster) and poplar (Populus tremula) for the production of polyphenolic extracts with antioxidant activity: aqueous extraction process using a twin-screw extractor and study of subcritical conditions."* [Online]. Available: https://theses.hal.science/tel-04233753v1.

[4] T. Popova and H. Hristova, "Trees of eternity-Pinus pinea L. in daily life, rituals, religion and symbolism. Archaeobotanical evidence from the territory of Bulgaria," *J Archaeol Sci Rep*, vol. 19, pp. 987–991, Jun. 2018, doi: 10.1016/j.jasrep.2017.06.012.

[5] B. Holmbom *et al.*, "Knots in trees - A new rich source of lignans," *Phytochemistry Reviews*, vol. 2, no. 3, pp. 331–340, Jan. 2003, doi: 10.1023/B:PHYT.0000045493.95074.a8.

[6] H. Sirén, "Current research on determination of medically valued stilbenes and stilbenoids from spruce and pine with chromatographic and spectrometric methods—A review," Nov. 01, 2024, *Elsevier B.V.* doi: 10.1016/j.jcoa.2024.100169.

[7] Z. Fang *et al.*, "Substituent effects on the ultraviolet absorption properties of stilbene compounds—Models for molecular cores of absorbents," *Spectrochim Acta A Mol Biomol Spectrosc*, vol. 215, pp. 9–14, May 2019, doi: 10.1016/j.saa.2019.02.072.

[8] A. Valletta, L. M. Iozia, and F. Leonelli, "Impact of environmental factors on stilbene biosynthesis," Jan. 01, 2021, *MDPI AG*. doi: 10.3390/plants10010090.

[9] E. S. Halmemies, H. E. Brännström, M. Karjalainen, J. Nurmi, and R. Alén, "Availability of extractives from various Norway spruce (Picea abies) stumps assortments," *Journal*

of Wood Chemistry and Technology, vol. 43, no. 1, pp. 13–27, 2023, doi: 10.1080/02773813.2022.2152049.

[10] T. Richard, A. Abdelli-Belhadj, X. Vitrac, P. Waffo Teguo, and J. M. Mérillon, "Vitis vinifera canes, a source of stilbenoids against downy mildew," *Oeno One*, vol. 50, no. 3, pp. 137–143, 2016, doi: 10.20870/oeno-one.2016.50.4.1178.

[11] H. Latva-Mäenpää, R. Wufu, D. Mulat, T. Sarjala, P. Saranpää, and K. Wähälä, "Stability and photoisomerization of stilbenes isolated from the bark of norway spruce roots," *Molecules*, vol. 26, no. 4, Feb. 2021, doi: 10.3390/molecules26041036.

[12] S. Navarro-Orcajada *et al.*, "Stilbenes: Characterization, bioactivity, encapsulation and structural modifications. A review of their current limitations and promising approaches," 2023, *Taylor and Francis Ltd.* doi: 10.1080/10408398.2022.2045558.

[13] B. De Filippis, A. Ammazzalorso, M. Fantacuzzi, L. Giampietro, C. Maccallini, and R. Amoroso, "Anticancer Activity of Stilbene-Based Derivatives," Apr. 20, 2017, *John Wiley and Sons Ltd*. doi: 10.1002/cmdc.201700045.

[14] V. Sáez *et al.*, "Oligostilbenoids in Vitis vinifera L. Pinot Noir grape cane extract: Isolation, characterization, in vitro antioxidant capacity and anti-proliferative effect on cancer cells," *Food Chem*, vol. 265, pp. 101–110, Nov. 2018, doi: 10.1016/j.foodchem.2018.05.050.

[15] H. Kim, K. H. Seo, and W. Yokoyama, "Chemistry of Pterostilbene and Its Metabolic Effects," Nov. 18, 2020, *American Chemical Society*. doi: 10.1021/acs.jafc.0c00070.

[16] D. Bonnefont-Rousselot, "Resveratrol and cardiovascular diseases," May 01, 2016, *MDPI AG*. doi: 10.3390/nu8050250.

[17] M. S. Ferreira, M. C. Magalhães, R. Oliveira, J. M. Sousa-Lobo, and I. F. Almeida, "Trends in the use of botanicals in anti-aging cosmetics," *Molecules*, vol. 26, no. 12, Jun. 2021, doi: 10.3390/molecules26123584.

[18] J. Gabaston *et al.*, "Separation and isolation of major polyphenols from maritime pine (Pinus pinaster) knots by two-step centrifugal partition chromatography monitored by LC-MS and NMR spectroscopy," *J Sep Sci*, vol. 43, no. 6, pp. 1080–1088, Mar. 2020, doi: 10.1002/jssc.201901066.

[19] J. Gabaston *et al.*, "Pinus pinaster Knot: A Source of Polyphenols against Plasmopara viticola," *J Agric Food Chem*, vol. 65, no. 40, pp. 8884–8891, Oct. 2017, doi: 10.1021/acs.jafc.7b04129.

[20] A. R. Suprun, A. S. Dubrovina, V. P. Grigorchuk, and K. V. Kiselev, "Stilbene Content and Expression of Stilbene Synthase Genes in Korean Pine Pinus koraiensis Siebold & Zucc," *Forests*, vol. 14, no. 6, Jun. 2023, doi: 10.3390/f14061239.

[21] R. Slimestad, "Amount of flavonols and stilbenes during needle development of Picea abies; variations between provenances," 1998.

[22] R. Bernini *et al.*, "A novel and efficient synthesis of highly oxidized lignans by a methyltrioxorhenium/hydrogen peroxide catalytic system. Studies on their apoptogenic and antioxidant activity," *Bioorg Med Chem*, vol. 17, no. 15, pp. 5676–5682, Aug. 2009, doi: 10.1016/j.bmc.2009.06.010.

[23] W. R., M. L. A. e Silva, R. C. Sola Veneziani, S. Ricardo, and J. Kenupp, "Lignans: Chemical and Biological Properties," in *Phytochemicals - A Global Perspective of Their Role in Nutrition and Health*, InTech, 2012. doi: 10.5772/28471.

[24] H. Satake, E. Ono, and J. Murata, "Recent advances in the metabolic engineering of lignan biosynthesis pathways for the production of transgenic plant-based foods and supplements," in *Journal of Agricultural and Food Chemistry*, Dec. 2013, pp. 11721–11729. doi: 10.1021/jf4007104.

[25] T. Umezawa, "Diversity in lignan biosynthesis," *Phytochemistry Reviews*, vol. 2, pp. 371–390, 2003, doi: 10.1023/B:PHYT.0000045501.58435.7e.

[26] Satake, H., Koyama, T., Bahabadi, S. E., Matsumoto, E., Ono, E., and Murata, J., "Essences in Metabolic Engineering of Lignan Biosynthesis," Metabolites, vol. 5, no. 2, pp. 270–290, May 2015, doi:10.3390/metabo5020270.

[27] S. Suzuki and T. Umezawa, "Biosynthesis of lignans and norlignans," *Journal of Wood Science*, vol. 53, no. 4, pp. 273–284, **Aug. 2007**, doi: 10.1007/s10086-007-0892-x.

[28] D. C. Ayres and J. D. Loike, "Determination of structure," in *Lignans*, Cambridge University Press, 2012, pp. 166–268. doi: 10.1017/cbo9780511983665.009.

[29] T. J. Schmidt, S. Hemmati, E. Fuss, and A. W. Alfermann, "A combined HPLC-UV and HPLC-MS method for the identification of lignans and its application to the lignans of Linum usitatissimum L. and L. bienne Mill," *Phytochemical Analysis*, vol. 17, no. 5, pp. 299–311, 2006, doi: 10.1002/pca.918.

[30] F. C. Schroeder *et al.*, "Pinoresinol: A lignol of plant origin serving for defense in a caterpillar," 2006. [Online]. Available: www.pnas.orgcgidoi10.1073pnas.0605921103

[31] J. Harmatha and L. Dinan, "Biological activities of lignans and stilbenoids associated with plant-insect chemical interactions," *Phytochemistry Reviews*, vol. 2, pp. 321–330, 2003.

[32] F. Cutillo, B. D'Abrosca, M. DellaGreca, A. Fiorentino, and A. Zarrelli, "Lignans and neolignans from Brassica fruticulosa: Effects on seed germination and plant growth," *J Agric Food Chem*, vol. 51, no. 21, pp. 6165–6172, Oct. 2003, doi: 10.1021/jf034644c.

[33] H. Nishiwaki, M. Kumamoto, Y. Shuto, and S. Yamauchi, "Stereoselective syntheses of all stereoisomers of lariciresinol and their plant growth inhibitory activities," *J Agric Food Chem*, vol. 59, no. 24, pp. 13089–13095, Dec. 2011, doi: 10.1021/jf203222w.

[34] S. Heinonen *et al.*, "In vitro metabolism of plant lignans: New precursors of mammalian lignans enterolactone and enterodiol," *J Agric Food Chem*, vol. 49, no. 7, pp. 3178–3186, 2001, doi: 10.1021/jf010038a.

[35] A. During, C. Debouche, T. Raas, and Y. Larondelle, "Among plant lignans, pinoresinol has the strongest antiinammatory properties in human intestinal Caco-2 cells," *Journal of Nutrition*, vol. 142, no. 10, pp. 1798–1805, Oct. 2012, doi: 10.3945/jn.112.162453.

[36] A.-C. Hopert, A. Beyer, K. Frank, E. Strunck, W. Wiinsche, and G. Volimer, "Characterization of Estrogenicity of Phytoestrogens in an Endometrial-derived Experimental Model," *Environ Health Perspect*, vol. 106, no. 9, pp. 581–586, Sep. 1998.

[37] C. Benassayag, M. Perrot-Applanat, and F. Ferre, "Phytoestrogens as modulators of steroid action in target cells," *Journal of Chromatography B*, vol. 777, no. 1–2, pp. 233–248, 2002, doi: 10.1016/S1570-0232(02)00340-9.

[38] S. O. Mueller, S. Simon, K. Chae, M. Metzler, and K. S. Korach, "Phytoestrogens and their human metabolites show distinct agonistic and antagonistic properties on estrogen

receptor α (ERα) and ERβ in human cells," *Toxicological Sciences*, vol. 80, no. 1, pp. 14–25, Jul. 2004, doi: 10.1093/toxsci/kfh147.

[39] P. Penttinen *et al.*, "Diet-derived polyphenol metabolite enterolactone is a tissue-specific estrogen receptor activator," *Endocrinology*, vol. 148, no. 10, pp. 4875–4886, Oct. 2007, doi: 10.1210/en.2007-0289.

[40] H. Adlercreutz, "Lignans and human health," *Crit Rev Clin Lab Sci*, vol. 44, no. 5–6, pp. 483–525, Sep. 2007, doi: 10.1080/10408360701612942.

[41] S. M. Mense, T. K. Hei, R. K. Ganju, and H. K. Bhat, "Phytoestrogens and breast cancer prevention: Possible mechanisms of action," *Environ Health Perspect*, vol. 116, no. 4, pp. 426–433, Apr. 2008, doi: 10.1289/ehp.10538.

[42] N. M. Saarinen, A. Wärri, R. P. M. Dings, M. Airio, A. I. Smeds, and S. Mäkelä, "Dietary lariciresinol attenuates mammary tumor growth and reduces blood vessel density in human MCF-7 breast cancer xenografts and carcinogen-induced mammary tumors in rats," *Int J Cancer*, vol. 123, no. 5, pp. 1196–1204, Sep. 2008, doi: 10.1002/ijc.23614.

[43] N. M. Saarinen, A. Abrahamsson, and C. Dabrosin, "Estrogen-induced angiogenic factors derived from stromal and cancer cells are differently regulated by enterolactone and genistein in human breast cancer in vivo," *Int J Cancer*, vol. 127, no. 3, pp. 737–745, Aug. 2010, doi: 10.1002/ijc.25052.

[44] N. M. Saarinen, A. Wärri, M. Airio, A. Smeds, and S. Mäkelä, "Role of dietary lignans in the reduction of breast cancer risk," *Mol Nutr Food Res*, vol. 51, no. 7, pp. 857–866, Jul. 2007, doi: 10.1002/mnfr.200600240.

[45] L. S. Velentzis, M. M. Cantwell, C. Cardwell, M. R. Keshtgar, A. J. Leathem, and J. V. Woodside, "Lignans and breast cancer risk in pre- and post-menopausal women: Meta-analyses of observational studies," *Br J Cancer*, vol. 100, no. 9, pp. 1492–1498, May 2009, doi: 10.1038/sj.bjc.6605003.

[46] L. S. Velentzis *et al.*, "Significant changes in dietary intake and supplement use after breast cancer diagnosis in a UK multicentre study," *Breast Cancer Res Treat*, vol. 128, no. 2, pp. 473–482, Jul. 2011, doi: 10.1007/s10549-010-1238-8.

[47] K. Buck, A. K. Zaineddin, A. Vrieling, J. Linseisen, and J. Chang-Claude, "Meta-analyses of lignans and enterolignans in relation to breast cancer risk," *American Journal of Clinical Nutrition*, vol. 92, no. 1, pp. 141–153, Jul. 2010, doi: 10.3945/ajcn.2009.28573.

[48] K. Buck *et al.*, "Estimated enterolignans, lignan-rich foods, and fibre in relation to survival after postmenopausal breast cancer," *Br J Cancer*, vol. 105, no. 8, pp. 1151–1157, Oct. 2011, doi: 10.1038/bjc.2011.374.

[49] A. K. Zaineddin *et al.*, "The association between dietary lignans, phytoestrogen-rich foods, and fiber intake and postmenopausal breast cancer risk: A german case-control study," *Nutr Cancer*, vol. 64, no. 5, pp. 652–665, Jul. 2012, doi: 10.1080/01635581.2012.683227.

[50] K. Buck *et al.*, "Serum enterolactone and prognosis of postmenopausal breast cancer," *Journal of Clinical Oncology*, vol. 29, no. 28, pp. 3730–3738, Oct. 2011, doi: 10.1200/JCO.2011.34.6478.

[51] J. Chen, J. K. Saggar, P. Corey, and L. U. Thompson, "Flaxseed and pure secoisolariciresinol diglucoside, but not flaxseed hull, reduce human breast tumor growth (MCF-7) in athymic mice," *Journal of Nutrition*, vol. 139, no. 11, pp. 2061–2066, Nov. 2009, doi: 10.3945/jn.109.112508.

[52] J. S. Truan, J. M. Chen, and L. U. Thompson, "Comparative effects of sesame seed lignan and flaxseed lignan in reducing the growth of human breast tumors (MCF-7) at high levels of circulating estrogen in athymic mice," *Nutr Cancer*, vol. 64, no. 1, pp. 65–71, Jan. 2012, doi: 10.1080/01635581.2012.630165.

[53] D. E. Barre *et al.*, "Flaxseed lignan complex administration in older human type 2 diabetics manages central obesity and prothrombosis - An invitation to further investigation into polypharmacy reduction," *J Nutr Metab*, vol. 2012, 2012, doi: 10.1155/2012/585170.

[54] S. Sirato-Yasumoto, M. Katsuta, Y. Okuyama, Y. Takahashi, and T. Ide, "Effect of sesame seeds rich in sesamin and sesamolin on fatty acid oxidation in rat liver," *J Agric Food Chem*, vol. 49, no. 5, pp. 2647–2651, 2001, doi: 10.1021/jf001362t.

[55] D. Nakano, C. Itoh, M. Takaoka, Y. Kiso, T. Tanaka, and Y. Matsumura, "Communications to the Editor Antihypertensive Effect of Sesamin. IV. Inhibition of Vascular Superoxide Production by Sesamin," *Biol Pharm Bull*, vol. 25, no. 9, pp. 1247–1249, 2002, doi: 10.1248/bpb.25.1247.

[56] M. Nakai *et al.*, "Novel antioxidative metabolites in rat liver with ingested sesamin," *J Agric Food Chem*, vol. 51, no. 6, pp. 1666–1670, Mar. 2003, doi: 10.1021/jf0258961.

[57] C. M. Liu, G. H. Zheng, Q. L. Ming, C. Chao, and J. M. Sun, "Sesamin protects mouse liver against nickel-induced oxidative DNA damage and apoptosis by the PI3K-Akt pathway," *J Agric Food Chem*, vol. 61, no. 5, pp. 1146–1154, Feb. 2013, doi: 10.1021/jf304562b.

[58] M. Galbe and G. Zacchi, "A review of the production of ethanol from softwood," *Appl Microbiol Biotechnol*, vol. 59, no. 6, pp. 618–628, 2002, doi: 10.1007/s00253-002-1058-9.

[59] S. Berthier, A. D. Kokutse, A. Stokes, and T. Fourcaud, "Irregular heartwood formation in maritime pine (Pinus pinaster Ait): Consequences for biomechanical and hydraulic tree functioning," *Ann Bot*, vol. 87, no. 1, pp. 19–25, 2001, doi: 10.1006/anbo.2000.1290.

[60] J. Gabaston *et al.*, "Pinus pinaster Knot: A Source of Polyphenols against Plasmopara viticola," *J Agric Food Chem*, vol. 65, no. 40, pp. 8884–8891, Oct. 2017, doi: 10.1021/acs.jafc.7b04129.

[61] Willför, S., Hemming, J., Reunanen, M., Eckerman, C., and Holmbom, B., "Lignans and Lipophilic Extractives in Norway Spruce Knots and Stemwood," *Holzforschung*, vol. 57, no. 1, pp. 27–36, 2003, doi: 10.1515/HF.2003.005.

[62] B. Holmbom *et al.*, "Knots in trees-A new rich source of lignans," *Phytochemistry Reviews*, vol. 2, no. 3, pp. 331–340, 2003, doi: 10.1023/B:PHYT.0000045493.95074.a8.

[63] J. Gabaston *et al.*, "Separation and isolation of major polyphenols from maritime pine (Pinus pinaster) knots by two-step centrifugal partition chromatography monitored by LC-MS and NMR spectroscopy," *J Sep Sci*, vol. 43, no. 6, pp. 1080–1088, Mar. 2020, doi: 10.1002/jssc.201901066.

[64] E. Saldívar-Guerra and E. Vivaldo-Lima, Eds., *Handbook of Polymer Synthesis, Characterization, and Processing*. Hoboken, NJ, USA: John Wiley & Sons, 2013. doi: 10.1002/9781118480793.

[65] Alfred. Rudin and Phillip. Choi, *The elements of polymer science and engineering*. Academic, 2013.

[66] G. Odian, *Principles of Polymerization*, 4th ed. Hoboken, NJ, USA: Wiley-Interscience (John Wiley & Sons), 2004. ISBN: 978-0-471-27400-1.

[67] P. M. M. Machado, T. F. Cruz, J. C. Bordado, and P. T. Gomes, "Controlled Radical Polymerization (ATRP and CMRP) of Vinyl Monomer Mediated by Cobalt(II/III) Complexes."

[68] H. Kubo, H. Nariai, and T. Takeuchi, "Multiple hydrogen bonding-based fluorescent imprinted polymers for cyclobarbital prepared with 2,6-bis(acrylamido)pyridine," *Chemical Communications*, vol. 3, no. 22, pp. 2792–2793, 2003, doi: 10.1039/b309917b.

[69] E. Oikawa, K. Motomi, and T. Aokl, "Synthesis and Properties of Poly (thioether Amide)s from 2,6-Bis (acrylamido) pyridine and Dithiols."

[70] A. Bzainia, E. Keller, A. Heeres, M. R. P. F. N. Costa, and R. C. S. Dias, "Synthesis of a dual-function monomer and its corresponding polymer for the valorisation of stilbenes from grape canes," *Eur Polym J*, vol. 236, Aug. 2025, doi: 10.1016/j.eurpolymj.2025.114142.

[71] A. Bzainia, G. Igrejas, M. J. V. Pereira, M. R. P. F. N. Costa, and R. C. S. Dias, "Purification of stilbenes from grape stems in a continuous process based on photo-molecularly imprinted adsorbents and hydroalcoholic solvents," *Sep Purif Technol*, vol. 349, Dec. 2024, doi: 10.1016/j.seppur.2024.127798.

[72] National Center for Biotechnology Information (NCBI), "Pinorisinol 4-O-glucoside," PubChem. Accessed: Jul. 27, 2025. [Online]. Available: https://pubchem.ncbi.nlm.nih.gov/compound/Pinoresinol-4-O-glucoside

[73] National Center for Biotechnology Information, "Pinoresinol diglucoside," PubChem. Accessed: Jul. 27, 2025. [Online]. Available: https://pubchem.ncbi.nlm.nih.gov/compound/Pinoresinol-diglucoside